

Lifetime of charmed particles (A review of experimental data)

A. O. Vaisenberg

Institute of Theoretical and Experimental Physics, Moscow
Usp. Fiz. Nauk **135**, 3-44 (September 1981)

The basic properties of charmed particles and of the cross sections for their production are briefly reviewed. The experimental data on lifetimes obtained up to the end of 1980 are discussed in detail. The corresponding experimental methods and proposals for future experiments are described.

PACS numbers: 14.40.Pe, 13.25. + m

CONTENTS

1. Introduction	733
a) Classification of charmed particles. b) Decay modes of charmed particles. c) Lifetime of charmed particles. d) Principal experimental data.	
2. Production of charmed particles	737
a) Production of charmed particles in deep inelastic interactions of neutrinos with nucleons. b) Production of charmed particles by photons. c) Production of charmed particles in strong interactions. 1) Beam-dump experiments; 2) decays of charmed particles in fast bubble chambers and streamer chambers; 3) experiments with composite emulsion chambers; 4) searches for decays in ordinary emulsion. d) Comparison of charmed-particle production probability in νp , γp , and pp interactions.	
3. Experiments on measurement of the lifetime of charmed particles	743
a) Experiments in neutrino beams. 1) The experiment FNAL E247; 2) the JINR-ITEP-Serpukhov experiment; 3) experiment FNAL E531; 4) the experiment FNAL E564: emulsion inside a 15-foot bubble chamber; 5) the experiment CERN WA17: emulsion in front of the BEBC chamber. b) The experiment with the Ω' spectrometer in a tagged photon beam. c) Measurements of lifetime at large Lorentz factors. d) Plans for new hybrid experiments. 1) The experiment of the Japan-Korea-Canada-USA Group; 2) hybrid experiment with fast bubble chamber as decay detector; 3) hybrid experiment with streamer chamber as decay detector. 4) Experiment with multilayer semiconductor live target.	
4. Accuracy and efficiency of target indications	747
5. Results of experiments on measurement of lifetime	748
a) The experiment FNAL E247 and searches for short decay times. b) Decays of D mesons. c) Decays of F^2 mesons. d) Decays of Λ_c baryons.	
6. Ratio of lifetimes $\tau_{D^{\pm}}/\tau_{D^0}$ in experiments in e^+e^- colliding beams	752
7. Conclusion	753
References	753

1. INTRODUCTION

a) Classification of charmed particles

After the discovery of the J/ψ particle^{1,2} and the ψ' particle in 1974 the existence in elementary particles of the long predicted quantum number charm^{4,5} became a reality. The family of new resonances with masses ≈ 3 GeV was interpreted as bound states of a system of a charmed quark and a charmed antiquark with total charm $C = 1 + (-1) = 0$. In experiments, carried out mainly in neutrino beams and electron-positron beams, it has been possible to observe particles with explicit charm $C = \pm 1$ and at the present time the existence of the new quantum number C appears to be as well proved as the existence of strangeness.

The set of new phenomena has been explained in the model of hadrons constructed of four quarks, each of which has three color states. The quarks have half-integer spin and baryon number $B = 1/3$; their other properties are given in Table I.

In the framework of SU(3) symmetry the quarks u , d , and s form a nonet of mesons (π^{*0-} , K^{*-} , K^0 , \bar{K}^0 , η , η'). The appearance of a fourth quark and the broadening of the symmetry group to SU(4) means that the nonet of $8 + 1$ pseudoscalar mesons must be supplemented by seven mesons: one of them, the η'_c meson, has hidden charm [$C = 1 + (-1) = 0$], and the other six—the D^* , D^0 , and F^* mesons and their antiparticles D^- , \bar{D}^0 , and F^- —have charm equal to $+1$ and -1 , respectively. Thus, the nonet of scalar mesons is extended to a hexadecuplet of $15 + 1 = 16$ states. They are shown in the three-

TABLE I. Basic properties of the four quarks.

Quark	Charge	Third component of isotopic spin I_3	Strangeness	Charm
u	2/3	1/2	0	0
d	1/3	-1/2	0	0
s	-1/3	0	-1	0
c	2/3	0	0	1

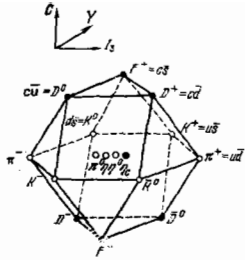


FIG. 1. (C, Y, I_3) diagram for the family of 16 pseudoscalar mesons.⁶ The quark composition of these mesons is shown in the diagram. In the plane $C=0$ there are 10 mesons, in the plane $C=1$ there are the three charmed mesons D^+ , D^0 , and F^+ , and in the plane $C=-1$ there are the three antiparticles D^- , D^0 , and F^- .

dimensional diagram of Fig. 1, where the quantities plotted along the axes are I_3 , C , and $Y=B+S$. The excited states D^* and F^* should have unit spin and negative parity. The quark composition of the charmed mesons is shown in the same diagram.

The number of predicted charmed baryons is 64.⁷ The family of 20 such baryons with spin and parity $1/2^+$ is shown in the I_3, C, Y diagram of Fig. 2. It forms a truncated tetrahedron, at the base of which is located the octet of "ordinary baryons ($p, n, \Lambda, \Sigma^{*0}, \Xi^{*0}$), which are composed of the quarks $u, d,$ and s . A classification of the remaining 12 baryons is given in Table II, where we have indicated the quark composition of the baryons and their designations from Fig. 2.

We note that the quark combinations cud and csu can be found in symmetric and antisymmetric states in the last two quarks. The theory therefore predicts the existence of four baryons with quantum numbers $C=1$ and $S=0$:

$$c(u\bar{d})_{\text{anti}}, \quad c(u\bar{d})_{\text{sym}}, \quad ddc \text{ and } uuc.$$

b) Decay modes of charmed particles

Charm C , like the strangeness quantum number S , is conserved in strong and electromagnetic interactions.

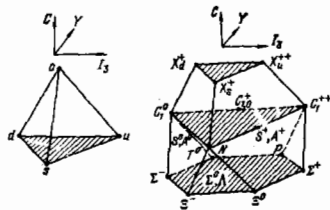


FIG. 2. (C, Y, I_3) diagram for the family of twenty baryons with spin $1/2^+$. The states of the three quarks u, d, s form the ordinary octet of $1/2^+$ baryons: $N(udd), P(udp), \Sigma^+(dds), \Sigma^0(uds), \Sigma^+(uus), \Xi^-(dds), \Xi^0(uss),$ and $\Lambda^0(uds)$, which is shown at the base of the diagram. There can be nine baryon states with one charmed quark (C); they are shown in the second plane of the tetrahedron. Baryon states with two charmed quarks (CC) contain one of the ordinary quarks $u, d,$ and s and form the triplet $uoc, dcc,$ and scs shown in the third cross-hatched plane of the diagram.

TABLE II. Charmed baryons with spin $1/2^+$.

Strangeness	$S=0$	$S=-1$	$S=-2$
Charm $C=2$	$X_u^{++} = ccu$ $X_d^{++} = ccd$	$X_s^+ = ccs$	
$C=1$	$C_1^+ = c(u\bar{d})_{\text{sym}}$ $C_1^0 = c(u\bar{u})$ $C_0^+ = c(u\bar{d})_{\text{anti}}$	$S^+ = c(su)_{\text{sym}}$ $S^0 = (csd)_{\text{sym}}$ $A^+ = c(su)_{\text{anti}}$ $A^0 = c(sd)_{\text{anti}}$	$T^0 = css$

Therefore charmed particles with large masses will "rapidly" go over to states of particles with the same C and S but with smaller masses, and the lightest of the charmed particles will decay as a result of the weak interaction, which does not conserve charm and strangeness. The weak-interaction Hamiltonian in the Weinberg-Salam theory has the form

$$H_W = \frac{G}{2} J J^+,$$

where the current J is equal to the sum of the charged and neutral currents $J = J_C + J_N$, which are respectively equal to:

$$J_C = (\bar{\nu}_e e) + (\bar{\nu}_\mu \mu) + u(d \cos \theta + s \sin \theta) + c(s \cos \theta - d \sin \theta),$$

$$J_N = (\bar{\nu}_e \nu_e) + (\bar{\nu}_\mu \nu_\mu) - (\bar{e} e) - (\bar{\mu} \mu) + (\bar{u} u) + (\bar{c} c) - (\bar{d} d) - (\bar{s} s).$$

It is easy to see that this Hamiltonian leads to the charmed-quark decay diagrams shown in Fig. 3. It follows from these diagrams that semileptonic decays of charmed particles will occur as the result of allowed transitions

$$c \rightarrow s \bar{\nu}_l$$

and forbidden transitions

$$c \rightarrow d \bar{\nu}_l \quad (\bar{\nu}_l = l^+ \nu_e \text{ or } \mu^+ \nu_\mu),$$

while nonleptonic transitions will occur as the result of the allowed transition

$$c \rightarrow s \bar{u} \bar{d},$$

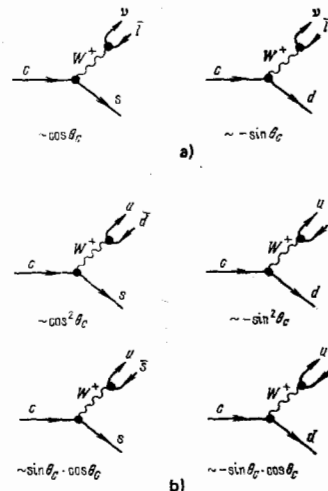


FIG. 3. Allowed transitions ($\sim \cos \theta$ and $\cos^2 \theta$), forbidden transitions ($\sim \sin \theta$), and highly forbidden transitions ($\sim \sin^2 \theta$) of the c quark. a) Semileptonic decays, b) decays of the c quark to uncharged quarks (hadronic decays).

the forbidden transitions

$$c \rightarrow us\bar{s}; \quad c \rightarrow ud\bar{d},$$

and the highly forbidden transition

$$c \rightarrow us\bar{d},$$

whose amplitudes are proportional to $\cos\theta$ or $\cos^2\theta$ and $\cos\theta \sin\theta$ or $\sin^2\theta$, respectively. In allowed transitions of charmed particles the selection rule $\Delta C = \Delta S$ applies. Thus, the allowed decay schemes of charmed mesons have the form

$$\begin{aligned} D^0 &\rightarrow (s\bar{l}) (K^- \dots), \\ D^0 &\rightarrow (\bar{K}, n\pi)^0, \\ D^+ &\rightarrow (s\bar{l}) (\bar{K}^0 \dots), \\ D^+ &\rightarrow (\bar{K}, n\pi)^+, \\ F^- &\rightarrow (s\bar{l}) (\eta, \eta', K\bar{K}), \\ F^+ &\rightarrow (\eta n\pi)^+, \quad F^+ \rightarrow (\eta' n\pi)^+, \\ F^+ &\rightarrow (K\bar{K}n\pi)^+. \end{aligned}$$

We note that in the allowed decays of D^0 and D^+ mesons, transitions with appearance of K^+ and K^0 mesons are forbidden, and in the decays of F mesons either there are no strange particles or particle-antiparticle pairs appear (K, \bar{K}).

c) Lifetime of charmed particles

The probability of semileptonic decays of charmed particles $\Gamma_{\nu l} = \Gamma$ (charmed particle $\rightarrow \nu + l + \text{hadrons}$) can be estimated from the known formula for the muon lifetime:

$$\Gamma_{\mu} = \frac{1}{\tau_{\mu}} = \frac{G^2 \mu^5}{192\pi^3},$$

if the muon mass μ is replaced by the quark mass M_c . Keeping in mind that $\tau_{\mu} = 2.27 \cdot 10^{-6}$ sec and $\mu = 0.106$ GeV, we obtain

$$\Gamma_{\nu l} = 3.4 \cdot 10^{16} M_c^5, \quad \text{where } M_c \text{ is in MeV.}$$

The existence of other decay channels increases the probability of decay of the c quark. In fact, in the simple quark model in which the decay probability is determined by the c quark and the second quark is a spectator, allowed decays occur as a result of the transitions

$$c \rightarrow s + e + \nu_e, \quad c \rightarrow s + \mu + \nu_{\mu} \quad \text{and} \quad c \rightarrow s + q + \bar{q}',$$

which are shown in the diagram of Fig. 3.

Thus, there exist five possible and equally probable decay channels (two leptonic and three color) and the total decay probability of the c quark turns out to be five times greater than Γ_{ν} , the lifetime being

$$\tau = M_c^{-5} \cdot 5.9 \cdot 10^{-12} \text{ sec.}$$

For $M_c = 2$ GeV the lifetime is $\tau_c = 2 \cdot 10^{-13}$ sec.

The direct means of measurement of such lifetimes consists of determining the distance from the point of creation of the particle to the point of its decay. This decay length l is related to the particle lifetime and its momentum as follows:

$$l = \frac{p}{M} \text{ sec.}$$

At momenta of the order of GeV/c the expected values of the decay lengths of charmed particles are tenths of

millimeters. Such lengths cannot be measured in large bubble chambers. The most appropriate method for measurement of them is nuclear emulsion. We recall that just this method has been successful in its time in measuring the lifetime of the π^0 meson, which is close to 10^{-16} sec.

d) Principal experimental data

The experimental data on charmed particles are given in Table III. This table is taken from the Review of Particle Properties,⁸ the reviews of Refs. 9 and 10, and supplemented by the results of the studies which are cited below. In the table we have given the values of the mass, isotopic spin I and G -parity, spin J and P -parity, the decay modes, and their relative probability.

The table begins with the D mesons ($M_{D^{\pm}} = 1868$ MeV, $M_{D^0} = 1863$ MeV), which form an isotopic doublet with a mass difference $M_{D^+} - M_{D^0} = 5.0 \pm 0.8$ MeV. The excited states of these mesons, the D^{*+} and D^{*0} mesons, have integral spin and a mass close to 2010 MeV. They drop rapidly to the ground state, emitting a photon or pion.

TABLE III. Properties of charmed particles.

Particle	$I^G(J^P)$	Mass, MeV/c ²	Decay mode	Relative probability in %
D^{\pm}	$\frac{1}{2} (0^-)$	1868.3 ± 0.9	$D^+ \rightarrow$ $e^+ \nu X$ $\bar{K} \pi^+ \pi^-$ (including $K^* \pi$) $\bar{K}^0 \pi^+$ $K^- X$ $K^+ X$ $\bar{K}^0 X$ $\bar{K}^+ X$ $\pi^+ \pi^+ \pi^-$ $K^+ K^- \pi^+$ $K^+ \pi^+ \pi^-$	8.2 ± 1.2 *) 3.9 ± 1.1 1.5 ± 0.6 10 ± 7 6 ± 6 39 ± 29 < 0.31 < 0.6 0.20
D^0, \bar{D}^0	$\frac{1}{2} (0^-)$	1863.3 ± 0.9	$D^0 \rightarrow$ $e^+ \nu X$ $K^- \pi^+ \pi^0$ $K^- \pi^+$ $K^- \pi^+ \pi^+ \pi^-$ $K^+ X$ $\bar{K}^0 X + K^0 X$ $\bar{K}^0 \pi^0 + K^0 \pi^0$ $\bar{K}^0 \pi^+ \pi^- + K^0 \pi^+ \pi^-$ $K^+ K^-$ $\pi^+ \pi^-$	8.2 ± 1.1 12 ± 6 1.8 ± 0.5 3.5 ± 0.9 35 ± 10 57 ± 26 < 6 4.4 ± 1.4 $(2.0 \pm 0.8) \cdot 10^{-1}$ $(5.9 \pm 3.2) \cdot 10^{-2}$
$D^{* \pm}$	$\frac{1}{2} (1^-)$	2008.6 ± 1.0	$D^{*0} \rightarrow$ $D^+ \pi^0$ $D^0 \gamma$	64 ± 11 28 ± 9 8 ± 7
D^{*0}		2006 ± 1.5	$D^{*0} \rightarrow$ $D^0 \gamma$	55 ± 15 45 ± 15
F^{\pm}	(0^-)	≈ 2040	$\bar{K}\bar{K}$ ϕX ηX $\eta' X$ $(X = e\nu, \mu\nu, n\pi)$ $F\gamma$	~ 100
$F^{* \pm}$	(1^-)	≈ 2140		
Λ_c^{\pm}	$\frac{1}{2} (1^+)$	2273 ± 6	$\Lambda_c^0 \pi^+ \pi^+ \pi^-$ $p\bar{K}^- \pi^+$ $p\bar{K}^+ \pi^-$ $\Delta (1232)^+ K^-$	
Σ_c^+		2457 ± 4	$\Lambda_c^+ \pi^0$ $\Lambda_c^+ \pi^+$	
Σ_c^{*+}	$\frac{1}{2} (1^+)$	~ 2430	$\Lambda_c^+ \pi^+$	

) This number refers to the mixture of (D^0, D^{-0}) and (D^+, D^-) mesons which consists of $56 \pm 3\%$ D^0 and $44 \pm 3\%$ D^+ in the region of ψ'' resonance (see section 6). The state X is mainly K and K^ .

After the D mesons the table gives the isotopic singlet of F^* mesons ($M_D = 2030$ MeV). Their excited states have a mass $M_{F^*} = 2140$ MeV. Transition of F^* mesons to the ground state is accompanied by emission of a photon.

Thus, the transitions of D^* and F^* states to the ground states of D and F mesons show that charm C, like strangeness S, is conserved in strong and electromagnetic interactions.

The decay schemes of the F mesons have been relatively well studied and are the best confirmation of existence of the new quantum number C. We see in the table the allowed semileptonic decays of D mesons, whose probability is close to 16.5%.¹⁾ This probability value is in agreement with the prediction of the theory. The hadronic decays shown in the table actually are divided into allowed and forbidden. For example, the probability of the allowed transitions $D^* \rightarrow K^0 \pi^+$ and $D^* \rightarrow K^- \pi^+ \pi^+$ amounts to $1.5 \pm 0.6\%$ and $3.9 \pm 1\%$, while for the probabilities of the forbidden transitions

$$D^+ \rightarrow K^+ \pi^+ \pi^-, \quad D^+ \rightarrow K^+ K^- \pi^+, \quad D^+ \rightarrow \pi^+ \pi^+ \pi^-$$

we know only upper limits of the probabilities, which are respectively 0.3, 0.6, and 0.2%. Another example is the probabilities of the forbidden transitions

$$D^0 \rightarrow K^+ K^-, \quad D^0 \rightarrow \pi^+ \pi^-.$$

They amount to only $2 \cdot 10^{-1}$ and $6 \cdot 10^{-2}\%$, respectively.

The decay modes of the F^* mesons have been less well studied. Almost all data on these decays have been obtained in experiments in e^+e^- colliding beams in analysis of the following events:

- (1) $e^+e^- \rightarrow K^+ K^- \pi + X,$
- (2) $\rightarrow K^+ K^- \pi^+ \pi^- + X,$
- (3) $\rightarrow K^+ \bar{K}^0 + X,$
- (4) $\rightarrow \gamma\gamma + \geq 2$ charged particles,
- (5) $\rightarrow \gamma\gamma + \gamma_e + \pi^\pm + X.$

In the last reaction γ_e is a photon of low energy $E_\gamma < 140$ MeV.²⁾ Events (1)–(3) have been studied in experiments carried out at Stanford in the e^+e^- beams SPEAR by means of the MARK I detectors, and events (4) and (5) in experiments with the DASP detector in the PETRA e^+e^- beams. The distribution of invariant masses of hadrons in reactions (1)–(3) shows a maximum in the region 2036–2044 MeV (23 events on a background of 7.3) and the mass value estimated from this maximum is

$$M_F = 2039.5 \pm 1.0 \text{ MeV}.$$

The invariant mass of the two photons in reaction (4) has an appreciable excess above background in the re-

- 1) The probability given in Table II for the decay $D \rightarrow e\nu X$ should be increased by a factor of two, since the decay $D \rightarrow \mu\nu X$ is equally probable.
- 2) It follows from conservation of isotopic spin that the F meson cannot decay by the channel $F^* \rightarrow F\pi$, but its mass is too low for the decay $F^* \rightarrow F\gamma$, in which a photon with energy $E_\gamma = 110$ MeV arises, is the only possible mode. This photon is used in reaction (5) as a marker for recognition of the F^* meson.

gion of the η -meson mass (at $E_{\text{cms}} = 4.42$ GeV).

The kinematics of the reaction (5) events, which were intended for detection of the excited state F^* , was balanced by means of the reaction

$$e^+e^- \rightarrow F^* F^{*\mp} \rightarrow (\pi^\pm \eta) (F^\mp \gamma),$$

and this balancing gave the distribution in the masses M_F and M_{F^*} shown in Fig. 4. For $E_{\text{cms}} = 4.42$ GeV we see six events grouped about the following mass values:

$$M_F = 2040 \pm 20 \text{ MeV} \quad \text{and} \quad M_{F^*} = 2150 \pm 50 \text{ MeV}.$$

Let us turn now to charmed baryons.³⁾ The best studied of these is the Λ_c^+ baryon. Its mass is less than the sum of the masses of the nucleon and the D meson; decay of the Λ_c baryon to these particles is impossible, and it decays as a result of the weak interaction into the states

$$\Lambda_c \rightarrow N K X \quad \text{or} \quad \rightarrow A X, \quad \text{or} \quad \rightarrow \Sigma X,$$

where X is a lepton pair or pions ($X = e\nu, \mu\nu, \text{ or } \pi\pi$). This particle has been observed in many studies,¹³⁻¹⁸ and in particular it was observed in experiments in e^+e^- colliding beams¹⁸ at $E_{\text{cms}} = 4.5$ GeV on the basis of a peak in the invariant-mass distribution of the hadrons ($pK^-\pi^+$) and ($\bar{p}K^+\pi^-$). This particle has been observed also in experiments with bubble chambers in neutrino beams produced in the proton accelerators.⁹ The mass value given in the table was obtained by averaging all these data.

Proof of the existence of the Σ_c^+ baryon shown in the table was obtained in Ref. 19, where the following event was observed in the BEBC bubble chamber exposed to a neutrino beam:

$$\nu + p \rightarrow \mu^- + p + K^- + \pi^0 + \pi^+ + \pi^+.$$

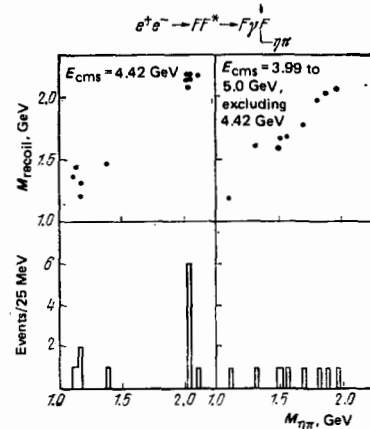


FIG. 4. Production of a pair of charmed mesons F, F^* in e^+e^- collisions. In the upper diagrams the mass ($\eta\pi^\pm$) is plotted as abscissa and the mass ($F^*\gamma$) is plotted as the ordinate; the lower histograms were obtained by projection of the points onto the axis of abscissas. Six events are located in the (F^* , F) region.

- 3) They are represented in Table III by three particles: Λ_c ($M = 2273$ MeV), Σ_c^+ ($M = 2457$ MeV), and the doubly charged baryon Σ_c^{++} ($M \approx 2430$ MeV).

ticles. We note that the probabilities of production of a charmed particle by photons and neutrinos differ by an order of magnitude (0.5% and 5%, respectively).

c) Production of charmed particles in strong interactions

Estimates of the cross sections for production of charmed particles in strong interactions have been obtained in two types of experiments: 1) beam-dump experiments,⁶⁾ in which the signature of production of charmed particles is the appearance of leptons arising from decay of charmed particles (so-called prompt leptons: neutrinos, electrons, or muons) and 2) direct experiments consisting of the direct observation of production and decay of these particles.

1) *Beam-dump experiments.* In these experiments the primary proton beam and all ordinary unstable hadrons whose decay is the source of neutrinos (π and K mesons, hyperons) are absorbed in a thick target of dense material (15–20 nuclear lengths). This target decreases the neutrino flux by 2000 to 3000 times in comparison with the conditions of an ordinary neutrino beam, but does not prevent observation of prompt leptons which arise in the target itself as the result of the decay of short-lived particles. The source of such leptons may be decay of charmed particles. Thus, measurement of the flux of leptons from a beam-dump target can give estimate of the cross section for production of these particles. The first experiments of this type at proton energy $E_p = 400$ GeV were carried out in the CERN proton synchrotron.^{39–41} In two experiments^{39,40} the neutrino detectors consisted of the large bubble chambers BEBC and Gargamelle located in the neutrino beam, and in the third experiment⁴¹ the detection of neutrino interactions was accomplished by the large neutrino detector of the CDHS Collaboration.⁷⁾ The arrangement of the targets and the three neutrino detectors can be seen in Fig. 5. The most important result of the experiments of Refs. 39 and 40 is that the fluxes of electron neutrinos and anti-neutrinos from the beam-dump target turned out to be large and of the same order as the fluxes of muon neutrinos. The data obtained in Ref. 41 with the large neutrino detector confirm, with significantly better statistics, the conclusion that there are prompt neutrinos.

We turn now to the experiments carried out at FNAL, in which direct muons and muon pairs were observed from a target bombarded by protons of energy 350 or 400 GeV. In these studies the beam-dump target was replaced by a "live" target⁸⁾ consisting of an ionization calorimeter. This provided the possibility of "seeing" interactions occurring in the target and measuring the

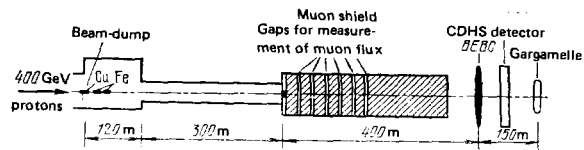
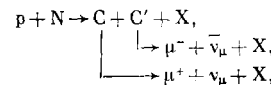


FIG. 5. First-generation beam-dump experiments of CERN. Prompt neutrinos were recorded by the BEBC and Gargamelle bubble chambers and by the neutrino detector of the CDHS Collaboration.

energy dissipated in it. By changing the target density it was possible to make measurements for different values of the average density. Extrapolation of the data to an infinitely high target density permits separation of the effect due to prompt muons from the background due to decays of π and K mesons. In Fig. 6 we have shown a diagram of one of these experiments.⁴⁵ The calorimeter-target consists of 49 iron plates of total thickness 2.44 m which can be moved so as to provide a decrease of the density of the calorimeter in comparison with the normal value by factors 1.75 and 2.5. Scintillation counters were located between the steel plates of the calorimeter. Beyond the calorimeter there was a muon range detector of weight 360 metric tons. To obtain a trigger pulse it was necessary to have a coincidence of an interaction in the calorimeter produced by the primary proton and the pulse from a muon penetrating at least 5.75 m of iron. As a result of the large size of the range detector, such a trigger efficiently selects all muons with momentum $p_\mu > 8$ GeV, i.e., almost all muons emitted into the forward hemisphere in the c.m.s.

The experiments of Refs. 43 and 44 were carried out in an appreciably more complicated arrangement consisting of the calorimeter described above, muon identifiers, and a toroidal magnetic spectrometer for measurement of the muon momentum.

In Ref. 44 measurements were made of the energy dissipated in the calorimeter with detection of prompt muons. If muon pairs arise in the semileptonic decays of charmed particles, for example, in the reaction



then neutrinos will carry away an appreciable fraction of the energy from the calorimeter. The results of these experiments are shown in Fig. 7, where as the abscissa we have plotted the calorimeter density (in

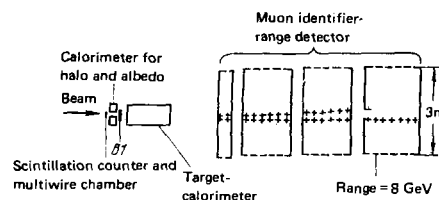


FIG. 6. Drawing of experiment of Ref. 45, in which detection of prompt muons occurred. A variable-density target-calorimeter replaces the beam-dump target. The energy of the muons is measured from their range.

⁶⁾ Russian term: Mishen'-svalka.

⁷⁾ The CDHS detector is the neutrino detector of the CERN-Dortman-Heidelberg-Saclay Collaboration. It contains 580 metric tons of iron and consists of a target, a hadron shower detector, and a magnetic spectrometer.

⁸⁾ A "live" target is one which permits observation of interactions occurring in it. A live target in which it is possible to record an interaction or decay vertex is sometimes called a vertex detector.

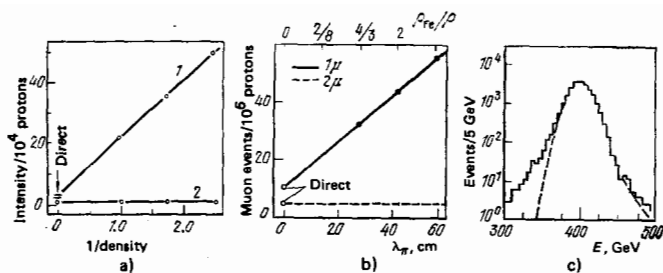


FIG. 7. Results of three experiments⁴³⁻⁴⁵ in which direct muons were recorded from a variable-density target-calorimeter. a) Direct muons in Ref. 45 (1—events with one and two muons when at least one of them has momentum $p_\mu > 8$ GeV/c; 2—events with two muons of different sign when the momentum of each muon is $p_\mu > 8$ GeV/c); b) direct single (—) and pair (---) muons in Ref. 43; c) distribution in energy ($E = E_{\text{calor}} + E_{\mu^+} + E_{\mu^-}$) for interactions with $\mu^+\mu^-$ pairs⁴⁴ (dashed lines—distribution in energy for ordinary proton interactions in the calorimeter. In dimuon events the neutrinos arising in decay of charmed particles carry away an appreciable fraction of the energy).

reciprocal units), and as the ordinate—the number of events with one or two muons. The remarkable result of these experiments^{43,44} is that the intensity of two-muon events I_2 does not depend on the calorimeter density, while the intensity of one-muon events I_1 decreases with increase of the density and when extrapolated to infinitely high density gives a value close to I_2 .

In Ref. 44 it was shown that a significant loss of the energy dissipated in the calorimeter is correlated with muon pairs. It follows from this that simultaneously with the muons there appear neutral particles (neutrinos) which carry away from the calorimeter a significant energy. This confirms the assumption that the observed prompt muons originated from semileptonic decays of charmed particles.

In 1979 the improved⁴⁷ second-generation experiments were completed at CERN. They were carried out with three lepton detectors: 1) the BEBC chamber, 2) the neutrino detector of the CDHS Collaboration, and 3) the neutrino detector of the CHARM Collaboration,⁹⁾ in which 100 metric tons of marble slabs were used as an absorber.

Assuming that, in all the experiments considered, the source of prompt muons is the decay of $D\bar{D}$ pairs, we can estimate the cross section for their production. The cross-section values obtained are given in Table V. In evaluation of the cross sections some uncertainty arises as the result of the need to use theoretical models for the production of the charmed particles, in order to accomplish the conversion from the limited phase space of the experiment to the total phase space of the inclusive process.⁴⁶

Consideration of the data given in the table shows that except for the very first experiments with bubble chambers as detectors of prompt neutrinos, which were of a

⁹⁾ CHARM is the CERN-Heidelberg-Aachen-Rome-Moscow Collaboration.

TABLE V. Cross section for production of charmed particles in beam-dump experiments and in experiments with a live target-calorimeter.

Reference	Lepton detector	Recorded leptons	$\sigma_{D\bar{D}}$, $\mu\text{b/nucleon}$
3 ^b	Bubble chamber Gargamelle	ν_τ, ν_μ	320^{+150}_{-120}
4 ⁰	Bubble chamber	Ditto	$100-400$
4 ¹	CDHS neutrino detector	" "	30
4 ³	Range muon identifier + toroidal magnetic spectrometer	μ^+, μ^-	13-60
4 ⁴	Ditto	μ^+, μ^- , and energy carried away by neutrinos	7-20 ¹⁾
1 ⁵	Range muon identifier	One-muon and two-muon events, $E_\mu > 8$ GeV	22 ± 9
Second-generation experiments			
4 ⁷	BEBC bubble chamber	ν_e	11 ± 2.1
4 ⁷	CDHS neutrino detector	ν_μ	22 ± 6.4
4 ⁷	CHARM neutrino detector	ν_μ	9.3 ± 4
4 ⁷	CHARM neutrino detector	ν_τ	11.4 ± 5.1
4 ⁷	CHARM neutrino detector	ν_μ	29 ± 9

qualitative nature and had poor statistics, all remaining experiments including the latest experiment with the BEBC bubble chamber give consistent results: the cross section for production of a pair of charmed particles by protons with energy 350-400 GeV turns out to be of the order of 10-30 $\mu\text{b/nucleon}$. Of course, it is not clear at present which charmed particles are responsible for the decays that we record in these experiments. They may be $D\bar{D}$ pairs or other pairs of charmed particles.

2) *Decays of charmed particles in a fast bubble chamber and streamer chamber.* The results described above were obtained by indirect methods. Recently they have been confirmed in two experiments in which it was possible to observe directly the decays of charmed particles arising in strong interactions. One experiment was performed at CERN by means of the fast bubble chamber,⁴⁸ and the other at FNAL with a streamer chamber as the decay detector.⁴⁹

The fast bubble chamber LEBC,¹⁰⁾ which is made of Lexan, has a volume of 1 liter, a diameter of 20 cm, a depth of 4 cm, and is filled with liquid hydrogen. The chamber is capable of 40 expansions per second, the diameter of the bubbles is close to 40-50 μm , and the average distance between bubbles in the track of a relativistic particle is about 100 μm . Thus, the resolution of the chamber is sufficient to measure decay lengths starting at a few tenths of a millimeter.

In a trial experiment with the LEBC chamber located in a beam of π^- mesons with energy 340 GeV ("slow" extraction, of duration 1.2 sec, during which time the chamber can accomplish about 48 expansions), it was possible to record associated decays of charmed particles. During ten days of operation in June and July of 1979 the chamber completed $1.3 \cdot 10^6$ expansions. A total of 110 000 photographs were obtained, which contained 48 000 interactions of π^- mesons with protons. Among these were found 20 events which are candidates for the pair production and decay of charmed particles

¹⁰⁾ LEBC is the Low European Bubble Chamber.

TABLE VI. Cross sections for production of charmed particles in direct experiments.

Reference	Method of detection of decays	Primary particles	σ_{cc}^+ , μb
48	Chamber (hydrogen filling)	π mesons, 350 GeV	If $\tau \sim 5 \times 10^{-13}$ sec, then $\sigma \approx 40 \mu\text{b}$
49	Streamer chamber	Protons, 350 GeV	If $\tau \sim 10^{-12}$ sec, then $\sigma \approx 20\text{--}50 \mu\text{b}$

(eight of them may be background) and eight three-prong forks which apparently represent D^* decays. For a charmed-particle lifetime $\sim 5 \cdot 10^{-13}$ sec these events correspond to a cross section for production of charmed-particle pairs $\sigma \sim 40 \mu\text{b}$ (Table VI). We note that the system contained no means for establishment of the nature of the secondary particles and therefore only a topological analysis of the events is possible.

In the experiment of Ref. 49 the live target in which the decay of charmed particles was observed was a small streamer chamber. Its dimensions were 4 cm along the beam, 3 cm width, and 0.45 cm height. The chamber operated at a pressure of 24 atm and was filled with a mixture Ne (90%)— H_2 . It was placed in a proton beam with energy 350 GeV (see Fig. 15) and triggered if there was a muon among the secondary particles. The experimenters succeeded in observing ten short-lived particles (on a background estimated as two particles) whose decay length was less than 10 mm, and the authors assume that these are charmed particles whose average lifetime lies between 10^{-13} and $2 \cdot 10^{-12}$ sec. Data on the production cross sections obtained in the two experiments are given in Table VI.

3) *Experiments with composite emulsion chambers.* Experiments carried out by the emulsion method can be divided into two groups: 1) experiments with composite emulsion chambers and 2) experiments with ordinary emulsion.

A diagram of one of the emulsion chambers is shown in Fig. 8.⁵³ It consists of a "target" and an "analyzer". The target consisted of 34 double emulsion layers,

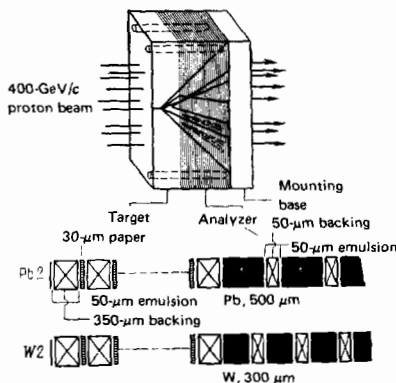


FIG. 8. Drawing of composite emulsion chamber. It consists of two parts: the target and the analyzer. In the analyzer, lead or tungsten foils are placed between the double emulsion layers, and its thickness is 7–8 radiation lengths. In the accelerator experiment the proton beam is directed perpendicular to the surface of the layers.

each double layer consisting of a lucite backing of thickness 350 μm covered on both sides with 50 μm of emulsion; the area of the layer is $12 \times 9.5 \text{ cm}^2$, and the total thickness of the target is 1.7 cm. The analyzer is made up of 80 layers of tungsten (or lead) foil of thickness 300 (500) μm and double emulsion layers deposited on a polystyrene substrate of thickness 150 μm . The thickness of the analyzer reaches 7–8 radiation lengths.

This chamber is easily capable of observation of intense shower jets arising in interaction of high energy particles with emulsion nuclei. Experiments with such chambers in cosmic rays were begun by the Japanese physicists already at the beginning of the 1960s.

We note the advantages and special features of the technique. Electrons and γ rays of high energy are found easily in such a chamber from the cascades arising in the foils of heavy material and recorded by the emulsion. The momentum of the charged particles is measured on the basis of the comparative multiple scattering in the lead or tungsten foils. This permits accurate measurements of momentum to be extended up to $\sim 10^9 \text{ eV}/c$. The beam of primary particles hits the emulsion perpendicular to its surface and, by following secondary particles from layer to layer one obtains not a continuous track consisting of a sequence of grains, but a sequence of tracks separated by a distance equal to the thickness of the substrate.

The first result of interest to us obtained by this method is from the year 1971.⁵⁰ In searches for shower jets produced by cosmic rays, a star accompanied by a strong electronic cascade was observed. Among the secondary particles of the star (Fig. 9) were found two tracks, each of which had a break (elbow), located at 1.38 and 4.88 cm respectively from the center of the star. After the elbow, which corresponds to an assumed decay, the tracks are followed for distances of the order of seven radiation lengths. Here no appreciable interactions were observed and consequently the tracks cannot belong to electrons. An electromagnetic shower from decay of a high-energy π^0 meson is spatially correlated with one of the breaks. The results of analysis of this decay are given in Table VII, where we have indicated the assumed decay scheme, mass of the decaying particle, and its lifetime.

A detailed discussion of this event is given in Ref. 51, where it is shown that its interpretation requires the

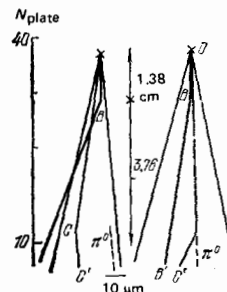


FIG. 9. Diagram of first event of production and decay of charmed particles. This event was observed in cosmic rays.

TABLE VIII. Analysis of first event of pair production of charmed particles.

Assumed decay mode	$Mx, \text{GeV}/c^2$	τ, sec
$X^0 \rightarrow \pi^0 + \pi^\pm$	1.78	$2.2 \cdot 10^{-14}$
$X^0 \rightarrow \pi^0 + p$	2.95	$3.6 \cdot 10^{-14}$

hypothesis of pair production of particles with a new quantum number.

The second case of pair production and decay of short-lived charged particles is described in Ref. 52, also carried out in cosmic rays. The masses of the two particles lie in the range 1.55–2.10 GeV/ c^2 , and their lifetimes are close to $6 \cdot 10^{-13}$ and $4 \cdot 10^{-12}$ sec. It is difficult, however, to extract from these data an estimate of the cross section for production of charmed particles. From this point of view the results obtained in the FNAL accelerator have great interest; here composite emulsion chambers were bombarded in a 400-GeV proton beam. Scanning revealed two events,^{54,55} which were interpreted as pair production of neutral particles and their decay. Analysis of the events shows that one of them can be the production of a pair of D^0 and \bar{D}^0 mesons or a pair of neutral charmed baryons, or associated production of a charmed meson and baryon. The second event is pair production of D^0 and \bar{D}^0 mesons. For the lifetime of these four neutral particles the following estimates are obtained:

$$\begin{aligned} \tau_1 &\approx (3-4) \cdot 10^{-14} \text{ sec}, & \tau_2 &\approx 1.2 \cdot 10^{-12} \text{ sec}, \\ \tau_3 &\approx (2.7-4.4) \cdot 10^{-13} \text{ sec}, & \tau_4 &\approx (2.8-4.2) \cdot 10^{-13} \text{ sec}. \end{aligned}$$

The two events discussed were observed in study of 1637 interactions of primary protons with emulsion nuclei. The authors give the following estimate for the cross section for associated production of charmed particles in proton-nucleon collisions:

$$\sigma(pp \rightarrow \bar{c}c) = \frac{2 \pm \sqrt{2}}{1637 (0.7)^2} \times 33 \cdot 10^3 = 80 \pm 60 \text{ } \mu\text{b/nucleon};$$

here $33 \cdot 10^3$ is the total cross section for proton-nucleon interaction, and 0.7 is a coefficient characterizing the detection efficiency. If we assume that the cross section for associated production is proportional to the mass number A , instead of $80 \pm 60 \text{ } \mu\text{b}$ we obtain $30 \pm 20 \text{ } \mu\text{b}$.

4) *Search for decays in ordinary emulsion.* In Refs. 56–62 a search was made for decays of charmed particles, with observation of forks or sharp bends of the trajectories in the immediate vicinity of stars produced by protons and pions of high energy. The search for decays was carried out in the forward cone of secondary particles at distances from a star not exceeding 0.6 mm. The selection of the stars was unbiased (only in Ref. 59 were interactions with a small multiplicity selected). In all these studies (104360 stars) no pair production of short-lived particles was observed. It follows from Ref. 56 that an upper limit of the cross section for pair or associated production of particles with a lifetime $\sim 3 \cdot 10^{-15} - 10^{-13}$ sec is $\sigma < 1.5 \text{ } \mu\text{b/nucleon}$ at the 90% confidence level.

The question arises: why were no cases of pair pro-

duction of charmed particles observed in these studies, although with cross sections of $\sim 10-50 \text{ } \mu\text{b/nucleon}$ the number of such particles should be of the order of ten?

This question is discussed in Ref. 63. The author concluded that the explanation is that the lifetime of charmed particles is either too small ($\tau < 10^{-15}$ sec) or too large ($> 10^{-12}$ sec). In the first case the decays are undistinguishable as the result of the shortness of the decay lengths, and in the second case the particles will leave the search zone without decaying. At the present time we know that the lifetimes of charged particles lie in a range $10^{-13} - 10^{-12}$ sec. The answer to the question raised may be that in strong interactions charmed particles are produced with relatively high energies, and as the result of the large value of the Lorentz factor they have long decay lengths. (The greater part of the searches in the studies mentioned in the table were carried out for decay lengths less than $300 \text{ } \mu\text{m}$.)

In some of the studies mentioned, candidates were found for decays of single charmed particles. To estimate the reliability of these events, we recall that the forward cone of secondary particles in which the search was made for decays is loaded by shower particles and Dalitz e^+e^- pairs from decay of π^0 mesons. For just this reason in Refs. 56 and 57 (78 000 stars) no forks or bends of the tracks with an opening angle or deflection angle $\theta < 3^\circ$ were discussed. The authors of these studies do not find it possible to state that the candidates for decay with an angle $\theta > 3^\circ$ found by them are real. Analysis shows that they can be explained by background of the following origin: "white" stars produced by a proton or neutron, pair production, decays of strange particles, and so forth. In Refs. 58–62 there were no restrictions on the angle θ . In Ref. 58 140 random stars were selected and 1400 secondary particle tracks were followed with a total length of 3.2 m. No candidates for decay of short-lived particles were observed.

In Ref. 59 at a distance of $194 \text{ } \mu\text{m}$ from the center of a star of the type $(1+4)p$ a V -shaped fork was observed with an opening angle of 2° . One track of the fork belongs to an electron, and the other to a hadron ($p_1 = 75 \text{ MeV}/c$, $p_2 = 9.1 \text{ GeV}/c$) and the authors discuss this event as a possible indication of leptonic decay of a charmed particle. Four candidates for leptonic decays were observed in Refs. 60 and 61 in a total statistics of 23 900 stars, and nine candidates for decays were observed in Ref. 62 in a statistics of 1120 stars. Summarizing, we note that all these cases of single production were obtained under conditions of high background, and separation of the effect from background and complete analysis of the events are impossible. These factors decrease the value of the information obtained: estimates of the cross sections for production and the lifetimes are hardly possible on the basis of these data.

d) Comparison of the probability of charmed particles in νp , γp , and pp interactions

We shall now consider the ratios

$$W = \frac{\text{charmed-particle production cross section}}{\text{total interaction cross section}}$$

which characterizes the probability of observing a charmed particle. Under the experimental conditions discussed above the quantity W has the following orders of magnitude:

Beam	W
Neutrinos	$\sim 5 \cdot 10^{-2}$
Photons	$\sim 5 \cdot 10^{-3}$
Protons	$\sim 10^{-3}$

It follows from these data that deep inelastic neutrino interactions turn out to be a more appropriate object for experiments on measurement of the lifetime. Of course, a deficiency of these experiments is the low cross section for production of charmed particles, which is close to 10^{-38} cm². This leads to a large mass of emulsion target, a long bombardment time, and as a consequence to accumulation of a substantial background of unrelated events. As will be seen below, it has turned out to be quite possible to accomplish target indication and lifetime measurement in photoproduction of charmed particles, while the solution of this problem for the strong interactions requires new experimental methods.

3. EXPERIMENTS ON MEASUREMENT OF THE LIFETIME OF CHARMED PARTICLES

a) Experiments in neutrino beams

We shall discuss here experiments which have been performed, which are being performed, and which are planned. In most experiments the target in which the production and decay of the charmed particles occurs is emulsion, except for two cases in which it is a fast bubble chamber and high-resolution streamer chamber. The secondary particles from the interactions and the particles which are decay products are analyzed by means of such detectors as multiparticle spectrometers or large bubble chambers. Particle trajectories established by the corresponding detector must be extrapolated to the emulsion target. The error in this extrapolation determines the region of target indication in which a search is made for the primary interaction and decays of the secondary particles. Thus, experiments with a vertex emulsion-target should combine the high resolution of emulsion for measurement of small decay lengths with the possibilities of modern methods of identification of decay particles on the basis of magnetic deflection, ionization, time of flight, behavior in an ionization calorimeter, in a muon identifier, in blocks of lead glass, and similar systems. We shall begin with experiments in neutrino beams, where almost all the data on charged-particle lifetimes have been obtained. We note that the first experiment which made it possible to see neutrino interactions in emulsion was carried out as long ago as 1964.⁶⁴

1) *FNAL experiment E247.*^{65,66} This experiment was carried out at FNAL in 1976–1978. It enabled us to see for the first time the decay of a charmed particle

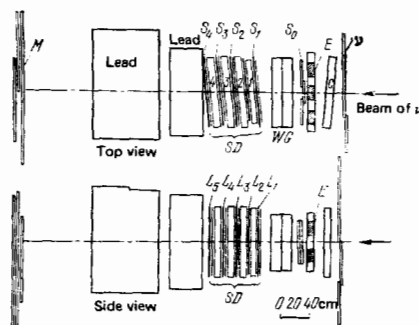


FIG. 10. Drawing of first experiment for measurement of lifetime of charmed particles.^{65,66} Shown are the emulsion target E consisting of 6 stacks, wide-gap spark chambers WG , shower detector SD consisting of layers of lead L and scintillators S , and muon identifier M .

in emulsion.^{65,66} The installation (Fig. 10) was in the same neutrino beam as the 15' bubble chamber, at a distance of 50 m from it, and consisted of an emulsion target and systems providing target indication and particle identification.

The emulsion (17 liters) was divided into six stacks made up of 1900 emulsion layers of area 7.3×20 cm² and thickness 600 μ m. The short side of the emulsion stack (7.3 cm) was directed along the beam, and the stacks were mounted on a massive slab of aluminum alloy. Beyond the emulsion, along the beam, was placed a target-indication system: wide-gap spark chambers WG (two gaps of width 15 cm each). Beyond these chambers there was a shower detector (four narrow-gap spark chambers 1–4 separated by scintillation counters S_{1-4} and layers of lead L_{1-5}) and a muon identifier which recorded muons emitted forward (in the direction of the neutrino beam) with momentum greater than 2 GeV/c (i.e., muons penetrating through two lead blocks located between the shower detector and the counters M).

For target indication, events were used in which at least two tracks could be seen in the wide-gap chambers WG which converged to a vertex located in the emulsion.

For each target indication an emulsion volume of about 1 cm³ was scanned at a magnification 20×15 . On the average this volume corresponded to two standard deviations in the coordinates of the projected interaction. Events found in this primary scanning were examined at a magnification of $750 \times$ for the purpose of analyzing relativistic tracks emitted forward.

In this work it was expected to obtain 230 ± 70 neutrino interactions in emulsion. The number of target indications obtained was 194. Of these the authors succeeded in observing in emulsion only 37. The average value of the scanned area per event found was 8.86 cm². The remaining 157 events were not found, although the total surface of emulsion investigated was 5360 cm² (34 cm² per unfound event).

2) *The JINR-ITEP-Serpukhov experiment.*⁶⁷ In this experiment the live target consisted of eight two-liter

emulsion stacks. The size of each stack was $10 \times 20 \times 10 \text{ cm}^3$. Target indication was accomplished with three-electrode spark chambers with 2.4 cm gaps and a working area $180 \times 230 \text{ cm}^2$. The target was placed in front of the ITEP neutrino detector, which consisted of a hadron calorimeter of spark chambers and a muon spectrometer with magnetized iron absorbers. The neutrino-generating target was bombarded by 7×10^{17} protons with energy of 70 GeV, and the expected number of interactions in the emulsion (of the charged-current type) was close to 60. In this experiment 20 target indications were obtained, on the basis of which eight neutrino stars were found in the emulsion. Following the secondary particles and searching near stars gave no indications of decays of charmed particles.

3) FNAL experiment E531.^{68,69} This experiment, which has yielded the greatest results, is being carried out by experimenters from Canada, Japan, Korea, and the USA.^{68,69} A diagram of the apparatus is shown in Fig. 11, where we can see the emulsion target and the composite system for target indication and particle identification, which consists of a magnetic spectrometer, a shower detector, a calorimeter, and a muon identifier. The 6-tesla magnetic field of the spectrometer is produced by an SCM-104 superconducting magnet. The particle trajectories in the spectrometer are recorded by drift chambers (12 chambers DCI at the entrance and eight chambers DCII at the exit of the spectrometer). The resolution of the drift chambers is $\sim 140 \mu\text{m}$, the momentum measurement accuracy is $\Delta p/p = 0.015 \pm 0.005p$ for particles passing through both systems of chambers and $\Delta p/p > 0.3p$ for particles emitted at large angles when only the first system of chambers and the fringing field of the magnet are used (p is in GeV/c). The shower detector is intended for measurement of the energy of γ rays arising from decay of π^0 mesons. It consists of 68 blocks of lead glass of dimensions $19 \times 19 \times 30 \text{ cm}^3$. The accuracy of measurement of the γ -ray energy is $\Delta E/E = 1.1/E^{1/2}$ (E is in GeV). The hadron calorimeter measures the total energy of charged and neutral hadrons. It consists of five layers of iron of thickness 10 cm separated by four vertical scintillators.

The muon identifier assures reliable separation of muons at momenta $p_\mu > 4 \text{ GeV}/c$. It contains two blocks

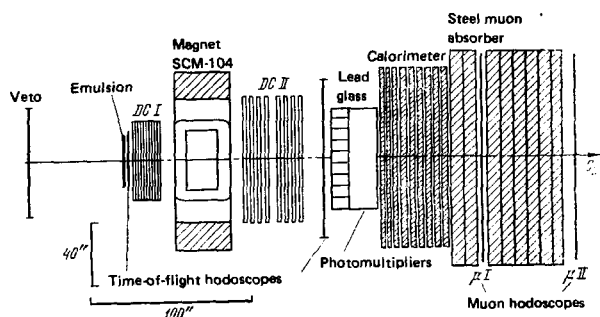


FIG. 11. Drawing of experiment E531.^{68,69} Shown are the emulsion target, magnetic spectrometer, calorimeter, wall of lead-glass counters, muon identifier, hodoscopic system of counters for measurement of time of flight and identification of muons.

of iron of thickness 1.2 and 2.9 m and scintillation hodoscopes located beyond the first and second blocks. The system for measurement of the time of flight has a resolution $1.60 \cdot 10^{-10} \text{ sec}$. It permits separation of π and K mesons with momentum up to $2.2 \text{ GeV}/c$ and identification of protons with momentum up to $4.5 \text{ GeV}/c$.

The emulsion target is made up of layers of two types: ordinary layers of thickness $600 \mu\text{m}$, and double emulsion layers. The latter consist of a thin ($70 \mu\text{m}$) polystyrene base on both sides of which emulsion layers ($830 \mu\text{m}$ each) have been deposited. The emulsion target contains 23 liters of emulsion included in a volume of $86 \times 71 \times 5 \text{ cm}^3$ and is divided into 39 modules, which can be removed for development as target indications are accumulated. The lower part of the target contains 27 modules with 68 double emulsion layers in each. The size of a module is $12 \times 9.5 \times 5 \text{ cm}^3$, and the modules are oriented in such a way that the neutrino beam is perpendicular to the surface of the double emulsion layers and parallel to the 5-cm edge of the module. The upper part of the stack consists of 12 modules (about ten liters of emulsion) made up of ordinary layers of area $5 \times 14 \text{ cm}^2$. In a module there are 177 such layers. The neutrino beam lies in the plane of the layers and is parallel to the 5-cm edge of the layer. A feature of the experiment is the presence of interchangeable double emulsion layers ($800 \mu\text{m}$ of polystyrene covered on both sides with $75 \mu\text{m}$ of emulsion layer). These layers are placed directly beyond the emulsion chamber (along the beam), and the plane of the layers is perpendicular to the neutrino beam. The target indication provided by the drift chambers gives the points of intersection of the trajectory with the interchangeable double emulsion layers. The background of particles from the emulsion forward is too high, and the possibility of changing layers reduces the accumulated background. The layers are changed approximately every two days, which reduces the background to ~ 2000 tracks per cm^2 . Four small, well collimated sources of Fe^{55} permanently located in each module produce small points on the interchangeable double emulsion layers and form a coordinate system fixed to the modules.

In this experiment the largest number of charmed-particle decays was recorded. With a target-indication efficiency close to 65%, up to the beginning of 1980, 685 interactions in the emulsion were observed. The region of the neutrino stars found was scanned as follows: search for neutral-particle decays was carried out in a cylinder of radius $300 \mu\text{m}$ and height $1000 \mu\text{m}$ (along the neutrino beam, from the center of the star); the second method of search was following trajectories from the point of exit from the emulsion backward to the star. Charged-particle decays were looked for in a cone of height 6 mm and half angle 0.2 radian, and also by following a track backward. In this experiment 18 uniquely identified events were found ($7D^0$, $5D^*$, $2F^*$, and $4\Lambda_c^+$), whose characteristics are given in Chapter 6.

We turn now to description of experiments in which

emulsion is used together with large bubble chambers.

4) FNAL experiment E564: *emulsion inside the 15-foot bubble chamber*. This experiment is being carried out by experimental groups from the USA, USSR, and Poland.⁷⁰ An emulsion is placed directly inside a 15-foot bubble chamber filled with deuterium. A special emulsion BR2 was prepared in the USSR for this experiment. It retains its sensitivity at cryogenic temperatures. The 22 liters of this emulsion were divided into 22 modules. Two soldered containers of stainless steel contained 11 modules each and were mounted on the entrance flange inside the chamber. A system of crosses on the container surface facing the chamber served to connect the coordinate systems of the chamber and the emulsion. Up to the middle of 1980 about 400 target indications were scanned in this experiment and from them 50 neutrino interactions in emulsion were found. Data obtained in this experiment on the decay of the charmed F meson⁷⁰ are given below in Table XII and in the caption to Fig. 18.

5) CERN experiment WA17: *emulsion in front of the BEBC chamber*.⁷¹⁻⁷⁴ A diagram of this experiment is shown in Fig. 12. Large stacks of Ilford K5 and G5 emulsion (3150 layers of area $20 \times 8 \times 0.06$ cm³; 10.5 liters in the first run, 20 liters in the second run) were mounted in front of the entrance window of the chamber, which operated with a hydrogen filling in a magnetic field of 3.5 teslas. The counter system VCS consisted of scintillation counters V and C and a multiwire proportional chamber (1024 wires). This chamber, which covered the entrance window of the BEBC, permits the coordinate system of the BEBC to be related to the emulsion coordinate system. For this purpose 2600 muons of high energy from the neutrino beam were passed through the BEBC chamber.

The location of the chamber D in the BEBC system (and correspondingly of the emulsion stacks in the BEBC system) was determined with an accuracy of 3 mm along the beam and 0.3 mm in the perpendicular directions. The counter system VCS also permitted establishment of the time correlation (on the basis of the time of flight) with the external muon identifier (EMI) of the BEBC chamber.

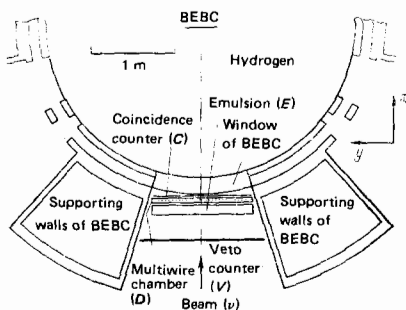


FIG. 12. Drawing of experiment with the BEBC chamber.⁷¹⁻⁷⁴ In front of the entrance window of the chamber, which is located in the neutrino beam of the large proton synchrotron at CERN, are placed an emulsion and a system of counters and multiwire chambers. The latter serve to relate the coordinate systems of the emulsion and the BEBC chamber.

In this experiment two bombardments were made in the wide-band neutrino beam of the large proton synchrotron. The neutrino spectrum of this beam has a maximum at 25 GeV and extends up to 150 GeV. During the bombardment about 10^{18} protons of energy 350 GeV hit the neutrino-generating target. During the experiment 206 000 photographs were scanned in a search for events in which at least three particles leave the wall of the BEBC chamber whose trajectories, when extrapolated to the emulsion, converge at a "point"; at least one of these particles must have a momentum greater than 3 GeV/c. The number of target indications obtained is 935, and of them 533 are due to charged currents (CC) and 412 to neutral currents (NC). The search for target indications was carried out for all CC events and for 60% of the NC events. In emulsion 214 interactions were found and eight charmed-particle decays were observed (three charged current and five neutral current). Two charged-particle decays are visible as sharp bends of the track (elbows). In four cases the decaying particles have been identified: three of them turned out to be D^0 mesons, and one a charmed charged baryon. The characteristics of these decays are given in Section 5.

b) Experiment with Ω' spectrometer in a tagged photon beam^{75,76}

In this experiment an emulsion was the target of the Ω' spectrometer at CERN (Fig. 13). The spectrometer operated in the tagged photon beam of the large proton synchrotron, with photon energies in the range 20–70 GeV. Single layers of emulsion were introduced into the photon beam by a mechanical device and removed from the beam after several accelerator pulses, corresponding to a dose of $\sim 10^6$ tagged photons. The emulsion layers were inclined at an angle of 5° to the beam, and thus the length of the beam in the emulsion was 6 mm. A total of about 6000 layers of dimensions $20 \times 5 \times 0.06$ cm were exposed (306 liters of BR2 emulsion). For target indication the controlling pulse of the spectrometer selected events with a charged-particle multiplicity of three or greater. In this experiment the spectrometer recorded a total of 160 000 events, and

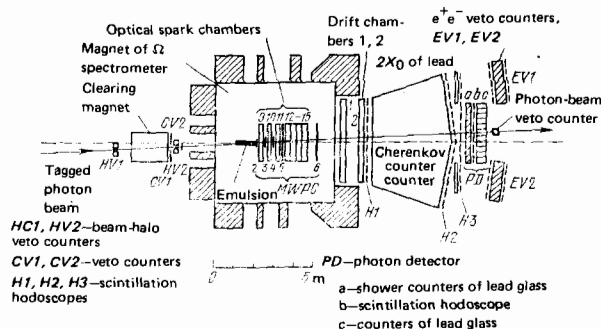


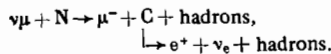
FIG. 13. Experiment in CERN tagged photon beam.^{75,76} Instead of a liquid-hydrogen target, the spectrometer includes an emulsion target consisting of emulsion layers. It is introduced into the beam mechanically and is removed after several accelerator pulses. The diagram shows spark chambers in the magnet gap, drift chambers at the magnet exit, a Cherenkov counter, and the photon detector-spectrometer.

1400 interactions were found in the emulsion. Thus, only a small part of the available material has been analyzed.⁷⁶

A remarkable result of this experiment is the fact that the greater part of the observed charmed particles arose in pair or associated production. One such event is shown in Fig. 14. Here a D meson and a Λ_c baryon were produced in the primary interaction of the photon with a nucleus. Reference 76 lists six cases of production of a pair of charmed particles. The summary tables in Section 6 give data on the lifetimes obtained in this experiment. (Only four particles out of 12 could be identified; six particles left no information in the Ω' spectrometer, and for the remaining two particles the information is insufficient to determine the mass and decay time of the particle.)

c) Measurements of lifetime at high Lorentz factors

The decay length is increased as the result of the relativistic time dilation and the decay path of a charmed particle can be measured in an ordinary bubble chamber if the particle energy is high. By this method it has been possible to measure the decay time of three charmed particles in the 15-foot FNAL bubble chamber in a neutrino beam (average energy $E_\nu \sim 90$ GeV). The charmed particles were identified on the basis of their semileptonic decay modes. For this purpose dilepton events with a μ meson and positron in the final state were selected. The source of such events is the reaction



Among 12 000 interactions of the CC type 89 dilepton events were selected, of which 54 were dimuon ($\mu^-\mu^+$) and 35 muon-positron (μ^-e^+).

In four events of the latter type near the neutrino interaction vertex another vertex can be seen which can be interpreted as the decay of a charmed particle. In one case a charged-particle decay can be seen, and in

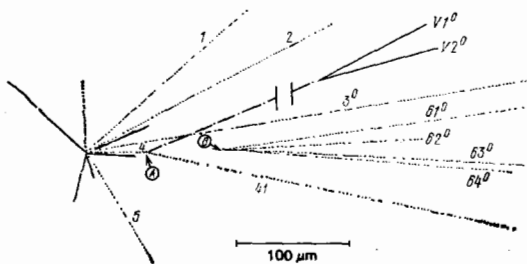


FIG. 14. Associated production of a charmed baryon and meson in the experiment with the Ω' spectrometer in a tagged photon beam. In the primary interaction of a photon with an emulsion nucleus two charmed particles are produced: a Λ_c^+ baryon and a D^0 meson. At distance of $50 \mu\text{m}$ from the primary star there is a decay $\Lambda_c^+ \rightarrow \Lambda^0 + \pi^+$. The decay of the Λ^0 hyperon (the invisible track of the neutral particle is shown by the dashed line) was recorded by the Ω' spectrometer. The D^0 meson decays at a distance of $124 \mu\text{m}$ from the star into four particles. The decay times (in units of 10^{-13} sec) are 0.88 ± 0.01 and 0.57 ± 0.02 for the D^0 meson and Λ_c^+ baryon, respectively.

two cases, neutral-particle decays. In the last (fourth) case the track of the decaying particle is obscured by a jet of particles and its charge cannot be established. The decay lengths lie in the range 6–11 mm and are measured with an accuracy 10–20%. The charged-particle decay is consistent with the scheme $D^+ \rightarrow e^+K^-\pi^+\nu$, and the two neutral particles are candidates for $D^0 \rightarrow K^-e^+\nu$ decays.

Bearing in mind that the decays found are a small part of the ensemble of 89 dilepton events for which the decay lengths are too short to be visible, the authors obtained the following estimates of the mean life of the charmed mesons:

$$\tau_+ = (2.5_{-1.5}^{+3.5}) \cdot 10^{-13} \text{ sec and } \tau_0 = (3.5_{-1.5}^{+3.5}) \cdot 10^{-13} \text{ sec}.$$

d) Plans for new hybrid experiments

We shall now discuss plans for experiments which are being prepared. They are intended for observation of decays of short-lived particles arising in strong and electromagnetic interactions.

1) *The experiment of the Japan-Korea-Canada-USA group.*⁷⁸ The success of experiment E531 made it possible to plan a more complex spectrometer to obtain better statistics on charmed-particle decays and to search for decays of B particles. The spectrometer consists of the usual elements: magnetic spectrometer, γ -ray detector, hadron calorimeter, toroidal magnetic spectrometer, and muon identifier. It will operate in a beam of high-energy pions, where the cross section for production of charmed particles is of the order of $10 \mu\text{b/nucleon}$ and the expected cross section for production of B particles is 2–3 orders lower. It is planned to use about 50 liters of emulsion, divided into modules of size $10 \times 10 \text{ cm}^3$ (*sic*) which will be successively, one after the other, exposed for 1–2 hours. The module is to be mounted on a precision table with electronic control which provides accurate displacement of the emulsion after several accelerator pulses in order that the entire surface of the emulsion stack be successively irradiated. The electronic part of the apparatus is to provide identification of the primary particle which produced the interaction and even spatial separation of the two vertices (interaction and decay). Ordinary drift chambers do not have sufficient resolution (the average distance between primary particle tracks in the beam is $\sim 40 \mu\text{m}$) and the success of this experiment will depend on silicon conductor detectors specially developed for this purpose.^{79, 80} They consist of a thin plate cut from a single crystal perpendicular to the $\langle 111 \rangle$ axis; on one surface of the plate is deposited a thin layer of gold, and on the other a thin layer of aluminum in which after etching it is possible to create conducting strips separated by $40 \mu\text{m}$. These detectors, 8 cm in diameter and 0.4 mm thick, should assure measurement in the spectrometer of track coordinates with an accuracy $\sim 20 \mu\text{m}$.

In this experiment, which will be started at the end of 1983, it is expected to measure more than 1000 decays of charmed particles and about 30 decays of B particles

if their production cross section is of the order of 100 nb.

2) *Hybrid experiment with fast bubble chamber as decay detector.*^{81, 82} In this project^{81, 82} a fast bubble chamber of the LEBC type is used as a live target for detection of decays in an experiment in the large European spectrometer EMS. The spectrometer provides accurate measurement of the momenta of the charged particles and the energy of the accompanying photons and is intended for study of multiparticle reactions. The hybrid system, which consists of the LEBC target-chamber and the EMS spectrometer, will operate in a beam of protons and pions with energy 350–400 GeV. The purpose of this experiment is to study the mechanism of production of charmed particles by hadrons and to measure their lifetime.

Apparently the use of fast bubble chambers will open new possibilities for study of the production and decays of short-lived particles in strong interactions.

3) *Hybrid experiment with a streamer chamber as decay detector.*^{49, 83} Another method of realizing a live target for observation of decays of charmed particles produced in strong interactions is a streamer chamber with high spatial resolution. In Ref. 49 it was possible with such a chamber to observe decays of charmed particles. We recall that a streamer chamber, with its short memory time and short dead time, permits electronic control with a complex and flexible trigger. It can operate in intense beams of charged and neutral particles and apparently after certain measurements it will be used successfully as a live target. The improvement of the resolution of the chamber is due to the decrease of the electron drift. For this purpose the gas pressure in the chamber will be taken up to 40 atm, the gas will be cooled, the delay time of the high-voltage pulse will be decreased, and the electron-optical part of the chamber will be improved. These measures will permit reducing the width of the tracks to $\sim 35 \mu\text{m}$. In the project which is being prepared at the present time the apparatus shown in Fig. 15 will be supplemented by a toroidal magnetic spectrometer for measurement of the muon momenta and by a composite system of hodoscopes and counters. This hybrid spectrometer is

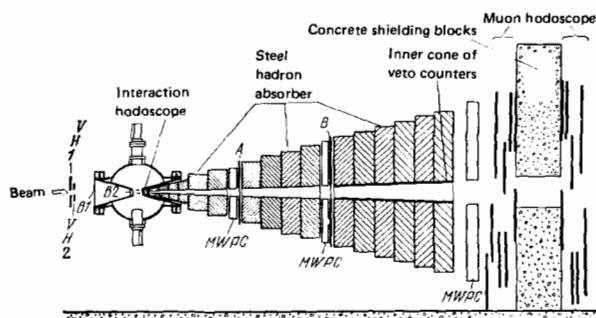


FIG. 15. Apparatus for observation of decays of charmed particles produced in interaction of protons with the gas of a streamer chamber. The controlling pulse was obtained from passage of a high-energy muon, produced in decay of a charmed particle, through the absorber.

planned for use in a neutron beam with intensity up to $\sim 10^8$ neutrons/pulse for the purpose of studying the production and decay of charmed particles and B particles.

4) *Experiment with multilayer semiconductor live target.*^{79, 80} We have mentioned above (paragraph 1 in subsection 3d) that the use of silicon semiconductor multiwire chambers will permit determination of particle coordinates in a spectrometer with an accuracy significantly better than that of drift chambers. Another use of such precision semiconductor detectors in the present problem is the construction of a live target consisting of several tens of semiconductor detectors joined in a stack. Each detector layer operates as an ionization chamber. The pulse height in the chamber is proportional to the number of relativistic particles which have passed through it and a target-stack of this type makes it possible to trace the increase of the number of charged particles from layer to layer and to recognize the layer in which a sudden increase occurred in the multiplicity, corresponding to a multiparticle decay. This method was used in the large magnetic spectrometer FRAMM at CERN, where photoproduction of charged particles is being studied. The first results obtained by this method consist of recognition in the spectrometer of multiparticle events which are due to the production and decay of charmed particles. A further development of the method will be the determination of the decay length from the number of the layer in which the ionization jump occurs.

4. ACCURACY AND EFFICIENCY OF TARGET INDICATIONS

We shall discuss here the question of the accuracy and efficiency of the target indications. Corresponding data on three experiments^{66, 68, 69, 72} are given in Table VIII, where we have shown the number of interactions predicted and found, the efficiency of the target indication (which is equal to the ratio of these numbers), and the accuracy of prediction of the coordinates of the point where the interaction occurred, as well as the emission angles of the secondary particles.

It follows from the table that the accuracies of prediction are approximately the same in all these experiments: the spread along the beam is close to ± 10 mm, and the spreads of the coordinates in the perpendicular directions are ± 1 mm; the spread in the predictions of the angles is close to 1–1.5%.

The efficiency of target indication in the experiments discussed is respectively 19, 20, and 64%. One of the causes of the loss of predicted events is the scattering

TABLE VIII. Accuracy and efficiency of target indication.

Reference	Number of interactions		Efficiency of target indication, %	Standard deviation, mm or degrees				
	predicted	found		Δx	Δy	Δz	$\Delta \theta$, depth	$\Delta \varphi$, azimuthal
66	194	37	19	10	1.2	1.4	~ 1.2	~ 1.0
72	770	214	28	8	1	1	~ 1.7	~ 1.5
68, 69	1077	685	64	8.5	0.95	0.70		
75, 76			~ 50				~ 1.5	~ 0.5

of particles in the emulsion block. In Ref. 66 the extension of the emulsion along the beam amounts to 7.3 cm, and in Ref. 67–10 cm. Dividing these values into four zones, we obtain the following distribution over the emulsion thickness of the interactions found:

→	4	10	9	14	7.3 cm
→	1	0	5	2	10 cm

In the second half of the chamber 30 interactions were found in the two experiments, and in the first half only 15. It follows from this that the role of scattering of particles is appreciable: only the second half of the chamber is working actively, and the extent of the emulsion along the beam should not exceed 3–4 cm. Another factor which influences the efficiency of the target indications (see Table IX) is the missing of “white” stars by the observer. A third cause is the number of tracks along which the target indication is made. For example, in 523 target indications in the BEBC chamber 169 interactions were found. This corresponds to a total efficiency $169/523 = 0.32$, and the efficiency depends on the number of tracks in the target indication in the following way: the efficiency is 0.14, 0.30, and 0.43 for a number of tracks 2, 3, and ≥ 4 , respectively.

Now let us consider data on the efficiency and accuracy of target indication in experiment E531. In order to check the technique, a special experiment⁸⁴ was carried out, for which a system consisting of an emulsion chamber, wire spark chambers, and scintillation counters was set up to imitate the conditions of experiment E531 (Fig. 16). The emulsion chamber consisted of 38 double emulsion layers (polystyrene substrate, 300 μm of emulsion deposited on both sides). The statistics of this trial experiment are as follows:

Number of controlling pulses 450.

Expected number of interactions 213 ± 25 .

Number of events reaching the reconstruction program and giving target indication 184.

As in experiment E531, the search for a predicted event was carried out by two methods:

1. A search over the volume, similar to the search used in all hybrid experiments.
2. Searching along the track.

The data obtained on the efficiency of target indica-

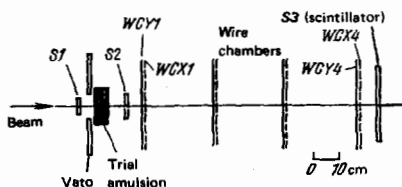


FIG. 16. Trial experiment which preceded experiment E531 and simulated its conditions. An emulsion stack is bombarded by a beam of pions, and target indication is accomplished by wire spark chambers.

TABLE IX. Results of search for interactions in a model of experiment E531.

Method	Volume search	Track search
Number of target indications Found	13	22
Of them $N_h = 0$	5	15
$1 \leq N_h \leq 3$	0	4
$N_h \geq 4$	5	7
Efficiency	40%	70%
Average time of search per event	16 hours	2 hours

tion are given in Table IX.

From this table it follows that the efficiency of scanning along the track reaches 70%, which is almost twice the efficiency of scanning over volume. The interactions found in scanning the volume have at least four highly ionizing particles, which indicates an appreciable loss of stars with a small number of tracks (“white” stars). We note that in experiment E531 (where the primary particles are neutrinos and the scanning is carried out in the backward direction along the secondary tracks) the corresponding scanning efficiencies are 40 and 80%, i.e., they agree with the efficiency of the trial experiment.

5. RESULTS OF EXPERIMENTS ON MEASUREMENT OF LIFETIME

a) FNAL experiment E247 and the search for short decay times

The first decay of a charmed particle produced by a neutrino in emulsion was found in Ref. 66. A diagram of the event, which was observed in spark chambers, is shown in Fig. 17. In the insert below this figure we have shown a diagram of the interaction in the emulsion: a star produced by a neutrino at point A, and a decay of a relativistic particle 4 at point B (which is located 182 μm from A) into three charged particle (tracks 41–43).¹¹⁾ The tracks of particles 1, 2, 3, 5, and 41 which are visible in the emulsion are also visible in the spark chambers (see Fig. 10). A K^0 decay in the second gap of the WG is correlated with this event (vertex V, tracks S1 and W1). Track 42 has a length of 3 mm and ends in the emulsion in a one-prong star, while track 41 passes through the shower detector without interaction. We can therefore assume that tracks 41 and 42 do not belong to electrons. Exact identification of tracks 41–43 is difficult, since eight months elapsed between preparation and development of the emulsion, but the authors consider the following to be most likely:

tracks 41 and 42 are π mesons or muons,
track 43 is a muon or a K or π meson.

The V^0 event visible in the second gap of the WG chamber is identified as the decay of a neutral particle—a hyperon or K meson. The momentum of these particles lies in the range 1.7–2.5 GeV/c, and the time of flight

¹¹⁾ The probability of decay in a distance up to 182 μm from the vertex of any of the known unstable particles does not exceed 10^{-6} .

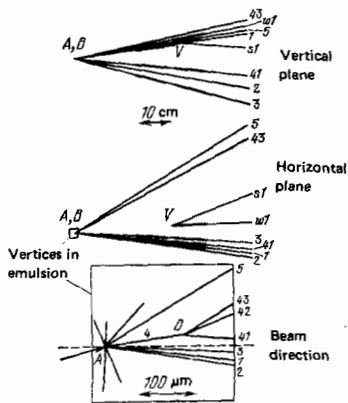
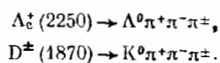


FIG. 17. First case of decay of charged charmed particle produced by a neutrino. In the upper part of the figure we have shown, in two projections, a drawing of the event in the spark chambers. In the insert at the bottom we have shown the events in the emulsion: the star at point A and the decay of charged particle 4 at point B into three particles. The interpretation of the decay is ambiguous. The decay length is $182 \mu\text{m}$ and the decay time is $\tau \sim 6 \cdot 10^{-13}$ sec.

is in the range (2–3.8) times the lifetime of Λ^0 and K_S^0 particles. A unique interpretation of this decay is impossible,¹²⁾ and the authors give only the following statements: assume that at point B a decay of charmed baryon or meson occurred:



An estimate of the mass of the decaying particle based on measurements in the chambers and the emulsion lies two and three standard deviations away from the indicated mass values, respectively, i.e., these hypotheses cannot be unconditionally refuted. We also cannot exclude the possibility of emission in the decay of an additional neutral particle (π^0 meson?) and the possibility that one of the secondary particles is a muon. An estimate of the decay time of the observed particle gives

$$\tau \approx 6 \cdot 10^{-13} \text{ sec.}$$

In this experiment an attempt was made to observe very short decay times by measuring the distance between the center of the star in the emulsion and the track of a shower particle "leaving" the star.⁸⁵ The authors analyzed 28 neutrino interactions in the emulsion. First they found the center of the interaction, defining it as the point from which the distance to the tracks of the shower particles is minimal. The zone of uncertainty found in this way in the emulsion plane lies in the range 0.05–0.10 μm in the direction perpendicular to the beam and in the range 0.1–0.5 μm along the beam.

Then, removing one shower track at a time from the star, they determined the new center of the star and the distance from this center to the removed track.⁸⁶ The total number of shower tracks in the 28 stars was

¹²⁾ In the summarizing tables (see below) it is listed in Table XIV among the ambiguously interpreted events.

close to 140 and with these statistics they observed no tracks with a deviation Δ from the center of the star exceeding three standard deviations. In 97% of the tracks the deviation from the center was $\Delta < 0.17 \mu\text{m}$. Analysis of the method carried out by the authors shows that a decay into charged particles would be observed if the lifetime of decaying particles was $\tau \geq 5 \cdot 10^{-15}$ sec.⁸⁸

b) Decays of D mesons

The results of all the hybrid experiments are given in the form of tables, in which are shown the decay length l , the sign of the charge and the momentum of the muon p_μ in the reaction $\nu + N \rightarrow \mu + C + X$, the decay hypothesis, the momentum p_c , the mass M_c , and the decay time τ_c of the charmed particle. In Table X we have shown all data on decays of neutral particles. In the following two Tables XI and XII we have collected data on the decays of eight charged particles identified as D^+ and F^+ mesons. In Table XIII we have given data on decays of charmed baryons, and in Table XIV—data on decays of particles which it has not been possible to identify uniquely.

Let us consider Table X with data on 13 D^0 decays. The first seven of these were obtained in experiment E531, the next three in the experiment with the BEBC chamber, and the last three in the experiment with the Ω spectrometer in a tagged photon beam.

The bold-face secondary particles (experiment E531) have been identified at a confidence level $> 90\%$. The neutral particles enclosed in parentheses have been predicted with a confidence level $> 99\%$. The lifetime values in the table were calculated for the mass $M_{D^0} = 1863 \text{ MeV}$.

Notes to Table X. 1) Decays No. 3, 4, and 7, which were tested for the hypothesis of decay of the D^* excited state, give the following mass value:

TABLE X. Decays of D^0 mesons.

No.	Reference	$l, \mu\text{m}$	$p_\mu, \text{GeV}/c$	Decay hypothesis	$p_c, \text{GeV}/c$	$M_c, \text{MeV}/c^2$	$\tau_c, 10^{-13} \text{ sec}$
1	88	27.2	+11	$\bar{D}^0 \rightarrow K^+ \pi^+ \pi^- \pi^0$	9.2	1766 ± 48	0.18 ± 0.02
2	88	116	-4	$D^0 \rightarrow K^- \pi^+ \pi^0 \pi^0$	30.1	1935 ± 132	0.24 ± 0.019
3	68	41	-10	$D^0 \rightarrow K^- \pi^+ \pi^+ \pi^0$	15.4	1855 ± 43	0.17 ± 0.013
4	68	67	-30	$D^0 \rightarrow \pi^- \pi^+ (K_S^0)$	11.3	1804	0.37 ± 0.035
5	68	6.5	-4	$D^0 \rightarrow K^- \pi^+ \pi^- \pi^+$	19.2	1923 ± 46	0.021 ± 0.003
6	88	2647	-26	$D^0 \rightarrow K^- \mu^+ (\nu)$	22.8 38.7		7.20 ± 0.367 4.24 ± 0.216
7	88	187	+34	$\bar{D}^0 \rightarrow K^+ \pi^- (\pi^0)$	6.8 9.5		1.71 ± 0.115 1.22 ± 0.082
8	72	54	-13.7	$D^0 \rightarrow \pi^- \pi^+ K^0$ $\pi^+ \pi^0 K^-$ $\mu^+ \nu_\mu K^-$	0.6 or 17 0.7 or 8.5 0.6 or 9.0		5.5 or 0.2 5.0 or 0.4 5.5 or 0.4
9	72	115		$D^0 \rightarrow \pi^- \pi^+ + K^0$ $\pi^+ \pi^0 K^-$ $\mu^+ \nu_\mu K^-$	3.1 or 17 3.0 or 11 23 or 11		2.3 or 0.4 2.4 or 0.7 2.5 or 0.7
10	72	182	-5.9	$D^0 \rightarrow \pi^- \pi^+ K^0$ $\pi^+ \pi^0 K^-$ $\mu^+ \nu_\mu K^-$	13 or 56 13 or 20 13 or 21		0.9 or 0.2 0.9 or 0.2 0.9 or 0.6
11	75	123		$\bar{D}^0 \rightarrow K^+ \pi^- \pi^-$		1866 ± 8	0.226 ± 0.005
12	76	124		$\bar{D}^0 \rightarrow K^+ \pi^+ \pi^-$			$0.86 \pm 0.01^*)$
13	76	267		$D^0 \rightarrow K^- \pi^+ \pi^0$	20 or 38		$0.45 - 0.85^{**})$

*) This decay was associated with the Λ_c^+ decay-event No. 6, in Table XIII.

**) This decay was associated with the D^- decay-event No. 6, in Table XI.

TABLE XI. Decays of D^+ mesons.

No.	Reference	$l, \mu\text{m}$	$p_{\mu}, \text{GeV}/c$	Decay hypothesis	$p_{\text{c}}, \text{GeV}/c$	$M_{\text{c}}, \text{MeV}/c^2$	$\tau_{\text{c}}, 10^{-13} \text{ sec}$
1	69	1802	-11	$D^+ \rightarrow K^- K^+ \pi^+ \pi^0$ $F^+ \rightarrow K^- K^+ \pi^+ \pi^0 (\pi^0)$	17.0 18.7	1862±25	6.60±0.17 6.53±0.33
2	69	2145	-7	$D^+ \rightarrow K^- \pi^+ \pi^+ (\nu)$ $F^+ \rightarrow \pi^- \pi^+ \mu^+ (\nu)$	16.1 13.0	—	8.33±1.03 11.19±0.16
3	69	457	$ p > 150$	$D^+ \rightarrow K^- K^+ \pi^+ \pi^0$ $F^+ \rightarrow K^- K^+ \pi^+ \pi^0$	10.1	1829±35 2011±33	2.82±0.09
4	69	2307	+7	$D^+ \rightarrow K^+ \pi^- e^+$ (ν)	9.4	—	15.3±1.68
5	69	13000	150	$D^+ \rightarrow K^- \pi^+ e^+$ (ν) $F^+ \rightarrow \pi^- \pi^+ e^+$ (ν)	11.8 101.5	—	6.86±0.69 8.66±0.76
6	76*)	94	—	$D^- \rightarrow K^0 \pi^+ \pi^- \pi^-$	6.6 10.3	—	0.88 0.57

*) This decay was associated with a D^0 decay—see decay No. 13 in Table X.

$$M(D^+ \pi^+) = 2007 \pm 13,$$

$$M(D^0 \pi^+) = 2010 \pm 3,$$

$$M(\bar{D}^0 \pi^-) = 2008 \pm 1 \text{ MeV}/c^2.$$

2) Decay No. 12 is associated with the decay of a Λ_c^+ baryon (see Fig. 14), and decay No. 13 with a D^- decay (see Table XI).⁷⁶

Some uncertainty in interpretation exists also in the data of this table: for example, for decays No. 4–6 we cannot completely exclude the hypothesis of decay of a neutral charmed baryon.

A peculiarity of the momentum values obtained for the decaying particles is their double value (decays No. 6–10). It arises as the result of the presence in the final state of a neutral particle and leads to two possible values of decay time.

We note that a probable choice between the two momentum values can be made from consideration of the spectrum of charmed mesons produced in neutrino interactions.

Let us consider the momenta of the mesons in those cases when they are determined uniquely. In Tables X–XIV we have given 12 such values and they are all greater than 9 GeV/c. Meanwhile in the table of D^0 -meson decays a choice is possible between $p_{D^0} < 3.1$ GeV/c and $p_{D^0} > 8.5$ GeV/c. The probability of repeated appearance of momenta less than 3 GeV/c is very small, and the higher momenta can be preferred to the smaller values.

On this assumption, averaging of the data of Table X gives for the lifetime of the D^0 meson the value

$$\tau_{D^0} \sim (0.4 - 0.6) \cdot 10^{-13} \text{ sec.}$$

In Ref. 68 the following estimates were obtained for τ_{D^0} (from decays No. 1–7 in Table X), which were made by the method of maximum likelihood (in units of 10^{-13} sec):

TABLE XII. Decays of F^+ mesons.

No.	Reference	$l, \mu\text{m}$	$p_{\mu}, \text{GeV}/c$	Decay hypothesis	$p_{\text{c}}, \text{GeV}/c$	$M_{\text{c}}, \text{MeV}/c^2$	$\tau_{\text{c}}, 10^{-13} \text{ sec}$
1	69	670	+30	$F^+ \rightarrow \pi^- \pi^+ \pi^+ \pi^0$	12.25	2026±56	3.70±0.12
2	69	130	not seen	$F^+ \rightarrow K^+ K^0 \pi^- \pi^-$	9.70	2089±121	0.91±0.12
3	70	50	-12	$F^+ \rightarrow \pi^+ \pi^+ \pi^- \pi^0$	> 2.32	2017±25	1.54

TABLE XIII. Decays of Λ_c^+ baryons.

No.	Reference	$l, \mu\text{m}$	$p_{\mu}, \text{GeV}/c$	Decay hypothesis	$p_{\text{c}}, \text{GeV}/c$	$M_{\text{c}}, \text{MeV}/c^2$	$\tau_{\text{c}}, 10^{-13} \text{ sec}$
1	72	354	-31.8 ±0.1	$\Lambda_c^+ \rightarrow p \pi^+ K^-$	3.72±0.04	2295 ±15	7.3±0.1
2	69	27.7	-59	$\Lambda_c^+ \rightarrow p \pi^+ \pi^- (\bar{K}^0)$	2.9 5.0	—	0.73±0.08 0.42±0.05
3	69	20.6	-41	$\Lambda_c^+ \rightarrow K^- p \pi^+ \pi^0$	2.23	—	0.70±0.07
4	69	40.6	-15	$\Lambda_c^+ \rightarrow \Lambda^0 \pi^+ \pi^- \pi^0$	5.73	2184±88	0.54±0.14
5	69	221	-8	$\Lambda_c^+ \rightarrow \Lambda^0 \pi^+ \pi^- \pi^0$	4.70	2382±90	3.58±0.29
6	76	50	—	$\Lambda_c^+ \rightarrow \Lambda^0 \pi^+$	6.73±0.23	2330±50	0.57±0.02*)

*) This decay, No. 6, was associated with a D^0 -meson decay; see decay No. 12 in Table X and Fig. 14.

$$\tau = 1.00^{+0.52}_{-0.31}, \quad \tau = 0.41^{+0.23}_{-0.13}, \quad \tau \approx 0.6.$$

For the first estimate all seven decays were used, and in the seventh decay the solution for the lower momentum was used, while in the sixth decay the solution for the higher momentum was used. In the second estimate decay No. 6 has been excluded, and in the last estimate the lower-momentum solution was taken in decay No. 6. (The probability that the decays 1–7 satisfy a single value of τ is only 1.3%, since the sixth decay gives too large a value of the decay time.)

Data on the decays of charged D^+ mesons are given in Table XI. In four of the five it is impossible to avoid their interpretation as F decays. However, this interpretation is unlikely (the background of F mesons for the five decays considered is 1.3). Application of the method of maximum likelihood to the five first decays gives

$$\tau_{D^+} = (10.3^{+10.5}_{-3.1}) \cdot 10^{-13} \text{ sec.}$$

Thus, comparison of τ_{D^+} and τ_{D^0} shows that the mean life of neutral charmed mesons is much less than that of charged charmed mesons. This conclusion follows also from a direct comparison of the decay lengths. This comparison makes sense if we make the reasonable assumption that the spectra of D^0 and D^+ mesons

TABLE XIV. Ambiguously interpretable decays.

Reference	$p_{\mu}, \text{GeV}/c$	$l, \mu\text{m}$	Decay hypothesis	$p_{\text{c}}, \text{GeV}/c$	$\tau_{\text{c}}, 10^{-13} \text{ sec}$
66	—	182	$\Lambda_c^+ \rightarrow \Lambda^0 \pi^+ \pi^- \pi^+$ $\Lambda_c^+ \rightarrow \Lambda^0 \pi^+ \pi^+ \pi^0$ $D^+ \rightarrow K^0 \pi^+ \pi^- \pi^+$ $D^+ \rightarrow K^0 \pi^+ \pi^+ \pi^0$	—	~ 6
73	-13	906	$D^+ \geq 4$ particles F^+	3.94–4.93	(1.6–5.3)
74	-4.77±0.01	96	$\Lambda_c^+ \rightarrow p + \pi^+ + K^-$ $F^+ \left. \begin{array}{l} 3 \text{ charged particles} \\ D_c^+ \\ \rightarrow 1 \text{ neutral particle} \end{array} \right\}$ $\Delta C = \Delta S$ or forbidden decays $D^+ \rightarrow K^+ K^- \pi^+$ $\Lambda_c^+ \rightarrow K^+ K^- p$ $\Lambda_c^+ \rightarrow \pi^+ \pi^- p$	—	~ 0.4–1.2
72	—	317 1559	Single-particle decays, kinematics do not agree with decay of a strange particle	—	—
76	—	32, 94 260, 341 685, 690 1900, 3332	8 decays of charged particles assigned to decays of D mesons	—	—

produced in neutrino interactions do not differ greatly. Then it follows from the data of Tables X and XI that

$$\langle l_{D^0} \rangle = 286 \mu\text{m}, \quad \langle l_{D^{\pm}} \rangle = 3940 \mu\text{m}.$$

We note that the decay lengths in decay No. 6 for D^0 mesons and decay No. 7 for D^{\pm} mesons are too great and agree poorly with the statistics of the remaining decay lengths. If these lengths are excluded, then

$$\langle l_{D^0} \rangle = 104 \mu\text{m}, \quad \langle l_{D^{\pm}} \rangle = 1680 \mu\text{m}.$$

The great difference in the average length of the decay path of neutral and charged mesons will not be removed by taking into account the different efficiency for detection of neutral and charged particles, although this factor will undoubtedly produce some shift of the data which is difficult to take into account.

Following the review article by Allasia⁷² let us discuss what is given by the data of the hybrid experiment with the BEBC chamber. The decay time $t = L/\beta c\gamma$ is determined uniquely from these data only for one decay of a Λ_c particle (decay No. 1 in Table XIII). In the remaining cases a kinematical analysis does not give a unique solution for the quantity $\beta\gamma$. However, in Refs. 87 and 88 it is shown that in a certain approximation, which is satisfied for eight decays obtained in this experiment, an estimate of τ is possible even if the value of β is unknown. In this method an estimate of τ is obtained from the distribution of the values of the distance Δ between the direction of emission of the secondary particle and the point where the interaction occurred. This quantity is given by $\Delta = L \sin\theta = t\beta c\gamma \sin\theta$, where θ is the angle between the vector L and the direction of emission of the secondary particle in the decay.

In the limit of high energy and large mass of an unstable particle ($\beta \rightarrow 1, \beta^* \rightarrow 1$) the quantity

$$\Delta = ct \operatorname{tg} \frac{\theta^*}{2}$$

(where θ^* is the emission angle of the secondary particle in the c.m.s.) does not depend on the value of β . To estimate the mean life by this method the authors assumed that the four charged particles whose decay was studied by them are D^{\pm} mesons, and the three neutral particles are D^0 mesons. The fifth charged particle included in the discussion as a D^{\pm} meson is the case observed in Ref. 66. The estimates obtained have the form

$$\tau_{\pm} = (2.5^{+2.2}_{-1.1}) \cdot 10^{-13} \text{ sec},$$

$$\tau_0 = (0.53^{+0.57}_{-0.21}) \cdot 10^{-13} \text{ sec},$$

$$\frac{\tau_{\pm}}{\tau_0} = 5^{+4}_{-3}.$$

Let us now consider the estimates of lifetime obtained in the experiment using the Ω' spectrometer in photo-production of charmed particles.^{75, 76} Application of the method of maximum likelihood to the three D^0 decays listed in Table X¹³⁾ gives

¹³⁾ In the case of decay No. 13 the value $(0.65 \pm 0.20) \cdot 10^{-13}$ sec was taken for the decay time, i.e., the center of the interval $(0.45 - 0.85) \cdot 10^{-13}$ sec.

$$\tau_0 = (0.58^{+0.8}_{-0.2}) \cdot 10^{-13} \text{ sec}.$$

Of the eight charged particles whose decay is recorded in this experiment, only one particle is identified with the D meson (event No. 6 in Table XI). Assuming that the remaining seven unidentified charged particles are D mesons,¹⁴⁾ and applying to these decays the method of estimation described above, the authors obtain

$$\tau_{\pm} \approx 4.4 \cdot 10^{-13} \text{ sec}.$$

c) Decays of F^{\pm} mesons

Almost all the decays listed in Table XI permit a second, probably less significant, interpretation as decays of F^{\pm} mesons. There are only three undoubted decays of F mesons, and they are given in Table XII. One of them, as we have mentioned, was obtained in Ref. 70. Corresponding drawings of the event in the emulsion and the chamber (in these drawings unrelated tracks have been removed) are shown in Fig. 18. Easily visible in the chamber are an electron-positron pair (tracks 5 and 6) and a positron from a second pair (track 7). Balancing of the kinematics of the event with two free parameters (a 2C fit) on the assumption that the decay $F^+ \rightarrow \pi^+ \pi^+ \pi^- \pi^0$ occurred, gives a F -meson mass $M_F = 2017 \pm 25$ MeV, with the mass of the system of three pions close to the ω -meson mass: $M(\pi^+ \pi^- \pi^0) = 808 \pm 20$ MeV. A 3C fit for a mass equal to the F -meson mass (2030 MeV) gives good agreement with the decay mode which was assumed.

Application of the method of maximum likelihood to the two other events shown in the table gives the following estimate:

$$\tau_F = (2.24^{+2.78}_{-1.05}) \cdot 10^{-13} \text{ sec}.$$

d) Decays of Λ_c baryons

In Table XIII we have given data on six decays of

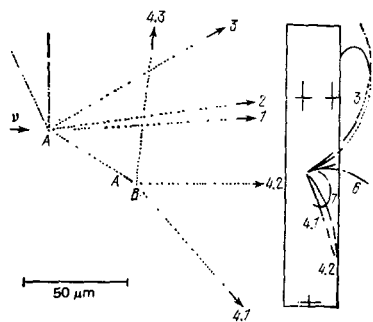
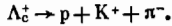


FIG. 18. Drawing of the event interpreted as decay of an F meson (see section 5, Table XII). Track 4 at a distance of $80 \mu\text{m}$ from the star splits up into tracks 41, 42, and 43. In the bubble chamber (extraneous tracks have been removed in the drawing) an e^+e^- pair is visible (tracks 5 and 6) and a positron track 7. The most likely decay is $F \rightarrow \pi^+ \pi^+ \pi^- \pi^0$.

¹⁴⁾ The decay lengths for these eight charged particles (see Table XIV) are respectively 32, 94, 260, 341, 685, 690, 1900, and 3332 μm .

charmed baryons. In the first of these, which was obtained in an experiment with the BEBC chamber, a track of a relativistic particle from a neutrino star at a distance of 354 μm from it breaks up into three relativistic tracks which with greatest probability belong to a K^+ meson, a proton, and a π^- meson. Thus, in this case the following decay scheme is possible:



The values of mass, momentum, and decay time for this and the remaining events are given in the table. Four of them were used in experiment E531 and the lifetime of the Λ_c baryon estimated for them is

$$\tau_{\Lambda_c} = (1.14_{-0.14}^{+0.90}) \cdot 10^{-13} \text{ sec.}$$

6. RATIO OF LIFETIMES τ_{D^\pm}/τ_{D^0} IN EXPERIMENTS IN e^+e^- COLLIDING BEAMS

Here we shall discuss estimates of the ratio of the lifetimes of charged and neutral D mesons obtained in experiments in electron-positron colliding beams at SPEAR in Stanford.⁹⁰⁻⁹²

This ratio can be obtained by measuring the relative probabilities of semileptonic decays of D^* and D^0 mesons. Indeed, in the transition



the change of isotopic spin is $\Delta T = 0$, and therefore there is equality in pairs of the widths of the corresponding decay channels of neutral and charged D mesons:

$$\begin{aligned} \Gamma(D^0 \rightarrow K^- e^+ \nu_e) &= \Gamma(D^+ \rightarrow \bar{K}^0 e^+ \nu_e), \\ \Gamma(D^0 \rightarrow \bar{K}^0 \pi^- e^+ \nu_e) &= \Gamma(D^+ \rightarrow K^- \pi^+ e^+ \nu_e) \end{aligned}$$

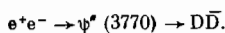
or, in general, summing over all channels:

$$\Gamma(D^0 \rightarrow e \nu X) = \Gamma(D^\pm \rightarrow e \nu X).$$

We shall use the designation $b = \Gamma(D - e \nu X) / \Gamma(D - \text{anything}) = \Gamma(D - D e \nu X) \tau$ for the relative probability of semileptonic decay of the D meson. Then obviously

$$\frac{\tau_{D^\pm}}{\tau_{D^0}} = \frac{b^+}{b^0}$$

—the ratio of the lifetimes of the D^* and D^0 mesons— is equal to the ratio of the coefficients b^+ and b^0 . Measurements of b^+ and b^0 were made by two methods. In both cases the energy of the colliding beams corresponded to the region of the ψ' resonance, $E_{c.m.s.} = 3770$ MeV, which is an intense and impurity-free source of $D\bar{D}$ pairs with contributions of the charged component D^* and the neutral component D^0 which have been studied:



In the first study, which was carried out in the MARK II apparatus,⁹⁰ those semileptonic decays of D particles were selected in which the decay of a pair particle was completely identified on the basis of hadronic decays. This permitted establishment of the charge state of the two particles. The values of b^+ and b^0 are

$$\begin{aligned} \text{for } D^+ \rightarrow e^+ + X, \quad b^+ &= (15.8 \pm 5.3) \% ; \\ \text{for } D^0 \rightarrow e^+ + X, \quad b^0 &= (5.2 \pm 3.3) \% . \end{aligned}$$

These values of the relative probabilities of semileptonic decays correspond to a ratio τ_+/τ_- (obtained by the method of maximum likelihood with inclusion of the fact that the useful and background events have a Poisson distribution):

$$\tau_+/\tau_- = 3.08_{-1.33}^{+4.1}.$$

The second method of measuring this quantity was carried out in the DELCO installation⁹⁰ and consists of comparing the frequency of appearance of one-electron and two-electron events N_1 and N_2 . Obviously N_1 is almost linear in b^+ and b^0 , while N_2 is quadratic in these variables:

$$\begin{aligned} N_1 &= A^+ 2b^0 (1 - b^0) + A^+ 2b^+ (1 - b^+), \\ N_2 &= A^+ b^0{}^2 + A^+ b^+{}^2. \end{aligned} \quad (*)$$

Here the coefficients $A^0(A^+)$ are equal to the product of the number of $D^0\bar{D}^0$ ($D^+\bar{D}^+$) decays by the detection efficiency. If the number of one-electron events N_1 and of two-electron events N_2 is measured and the coefficients A are known, then it is possible to find a solution for b^0 and b^+ and consequently also the ratio τ^+/τ^- . The system of equations (*), however, has two solutions and a choice between them is made on the basis of the additional consideration that in $D^+ - D^+$ decays neutral kaons K^0 arise, and in D^0 decays—charged kaons. This study found $N_1 = 734$ and $N_2 = 21$ (background about 5) electron events and the quantities b^0 and b^+ have the following values:

$$b^0 < 4\%, \quad b^+ = 22.0_{-2.2}^{+4.4}\% \text{ (at the 95\% confidence level),}$$

from which, using the method of maximum likelihood,

$$\tau_+/\tau_0 > 4.3 \text{ (at the 95\% confidence level).}$$

TABLE XV. Results of measurement of lifetime of charmed particles (in units of 10^{-13} sec).

Experiment	E531 ^{88, 89*}	BEBC ⁷¹⁻⁷⁴	SPEAR ^{80, 81}	Ω' spectrometer, Refs. 75, 76
Result:				
τ_{D^0}	$1.0_{-0.34}^{+0.52}$	$0.53_{-0.25}^{+0.57}$		$0.58_{-0.12}^{+10.8}$
τ_{D^\pm}	$10.3_{-4.1}^{+10.5}$	$2.5_{-1.1}^{+2.2}$		~ 4.4
τ_F	$2.24_{-1.05}^{+2.78}$			
τ_{Λ_c}	$1.14_{-0.44}^{+0.90}$			
τ_{D^\pm}/τ_{D^0}	≈ 10	5_{-3}^{+6}	$3.08_{-4.33}^{+4.1}$	≈ 8
			> 4.3	

*) As a result of the increase in statistics in experiment E531 which occurred in the last half year, the lifetime estimates given in the first column of the table have changed slightly. The new estimates have the following values¹⁰⁰:

$$\begin{aligned} \tau_{D^0} &= 3.1_{-0.7}^{+1.1}, \quad \tau_{\Lambda_c} = 1.7_{-0.5}^{+0.9} \\ \tau_{D^\pm} &= 9.5_{-3.3}^{+6.5}, \quad \tau_F = 2.0_{-0.8}^{+1.8} \end{aligned}$$

Thus, the ratio τ_{D^\pm}/τ_{D^0} in experiment E531 has changed from a value ~ 10 to a value ~ 3 as the result of an increase of the D^0 -meson lifetime. This result does not change the general conclusion that there is a difference in the lifetimes of the D^* mesons and the remaining charmed particles, which is based on consideration of the whole set of experimental data.

If we use the theoretical value⁹³

$$\Gamma(D \rightarrow K\pi) = 1.4 \cdot 10^{11} \text{ sec}^{-1},$$

which was obtained by analogy with the width $\Gamma(K \rightarrow \pi e \nu)$ with a small uncertainty due to form factors, then from form factors, then from the values of b^0 and b^* obtained it follows that the lifetimes of the D^* and D^0 mesons are

$$\tau_{D^*} < 2.1 \cdot 10^{-13} \text{ sec},$$

$$\tau_{D^\pm} = (10.4^{+2.3}_{-2.0}) \cdot 10^{-13} \text{ sec at the 95\% confidence level.}$$

Thus, these results are in agreement with the data obtained in hybrid experiments with an emulsion target in neutrino or photon beams.

In conclusion we give Table XV as a summary of measurements of lifetimes of charmed particles and of the ratios of lifetimes of charged and neutral particles.

7. CONCLUSION

We have discussed the data on measurement of the lifetime of charmed particles produced in beams of neutrinos, photons, and hadrons. It follows from this discussion that hybrid experiments with vertex targets, which combine the possibilities of accurate measurement of the decay lengths, identification of the secondary particles, and reconstruction of the decay scheme, will permit detailed data to be obtained on the lifetime of charmed particles. Increase of the accuracy and efficiency of target indication in such experiments together with the appearance of new "live" targets such as fast bubble chambers or streamer chambers will permit investigation of the lifetimes of charmed particles produced in strong interactions and, possibly, advancement to study of the lifetimes of B particles.

It is appropriate to raise the question of what kind of track detector should be used with a live target: what should be given preference—bubble chambers or composite spectrometers. Apparently the future belongs to the latter. One of the reasons for the low efficiency of target indication in experiments with bubble chambers is the superposition of unrelated tracks. The high time resolution possible in spectrometers leads to a significant increase of the scanning efficiency.

The physical results obtained can be summarized in general form as follows: 1) pair production and decay of charmed particles have been observed. 2) The lifetime of charmed particles lies in the range 10^{-12} – 10^{-13} sec. 3) The lifetime of D^* mesons is almost an order of magnitude greater than the lifetime of D^0 mesons. 4) The lifetime of other charmed particles is close to the lifetime of D^0 mesons.

These results confirm the prediction of the theory that the lifetime of charmed particles is close to 10^{-13} sec but indicate the inadequacy of the simple quark-spectator model, according to which $\tau_{D^*} = \tau_{D^0} = \tau_{F^*}$.

The scope of the review does not include theoretical studies, in which attempts have been made to explain the reason for this inconsistency. We shall point out, however, that the possibility of this difference in the lifetimes has been discussed by many authors^{94, 92–95} and

that at the present time there is an extensive literature on this question. This literature indicates that, since calculations of the probability of the semileptonic decay modes agree more or less accurately,⁹³ the difference in the lifetimes can arise most likely from the nonleptonic part of the interaction Hamiltonian: in order to predict the lifetime of charmed particles it is necessary to know how quarks recombine into hadrons. This is a difficult problem, which includes the dynamics of strong interactions.^{96–104} It is evident that the experimental and theoretical solution of the problem of charmed-particle lifetimes will require great effort from experimenters and theoreticians.

The author thanks L. B. Okun', M. I. Adamovich, V. A. Smirnitkii, I. S. Tsukerman, and M. I. Daion, who have read this review, for their critical remarks and discussion.

- ¹J. Aubert *et al.*, Phys. Rev. Lett. **33**, 1404 (1974). J. Augbert *et al.*, Phys. Rev. Lett. **33**, 1624 (1974).
- ²J. Augustin *et al.*, Phys. Rev. Lett. **33**, 1406 (1974).
- ³G. Abrams *et al.*, Phys. Rev. Lett. **33**, 1453 (1974).
- ⁴J. Bjorken and S. Glashow, Phys. Lett. **11**, 255 (1964).
- ⁵S. Glashow, J. Nopoulos, and L. Maiani, Phys. Rev. **D2**, 1285 (1970).
- ⁶M. Gaillard, B. Lee, and J. Rosner, Rev. Mod. Phys. **47**, 277 (1975).
- ⁷V. I. Zakharov, B. L. Ioffe, and L. B. Okun', Usp. Fiz. Nauk **117**, 227 (1975) [Sov. Phys. Usp. **18**, 757 (1975)].
- ⁸Review of Particle Properties, Rev. Mod. Phys. **52**, No. 2, Part II, S1, (1980).
- ⁹J. Kirkby, SLAC-PUB-2419, 1979.
- ¹⁰J. Dorfan, SLAC-PUB-2429, 1979.
- ¹¹D. Lüke, SLAC-PUB-2028, 1978.
- ¹²R. Brandelik *et al.*, Z. Phys. **C1**, 233 (1979); Phys. Lett. **B80**, 412 (1979).
- ¹³A. Cnops *et al.*, Phys. Rev. Lett. **42**, 197 (1979).
- ¹⁴C. Baltay *et al.*, Phys. Rev. Lett. **42**, 1721 (1979).
- ¹⁵K. Giboni *et al.*, Phys. Lett. **B85**, 437 (1979).
- ¹⁶D. Drijard *et al.*, Phys. Lett. **B85**, 452 (1979).
- ¹⁷W. Lockman *et al.*, Phys. Lett. **B85**, 443 (1979).
- ¹⁸G. Abrams *et al.*, Phys. Rev. Lett. **44**, 10 (1980).
- ¹⁹M. Calicchio *et al.*, Phys. Lett. **B93**, 521 (1980).
- ²⁰E. Gazzoli, Phys. Rev. Lett. **34**, 1125 (1975).
- ²¹B. Knapp, Phys. Rev. Lett. **37**, 882 (1976).
- ²²C. Baltay, Phys. Rev. Lett. **42**, 1721 (1979).
- ²³A. Benvenuti *et al.*, Phys. Rev. Lett. **34**, 419 (1975).
- ²⁴A. Benvenuti *et al.*, Phys. Rev. Lett. **35**, 1199 (1975). A. Benvenuti *et al.*, Phys. Rev. Lett. **35**, 1203 (1975).
- ²⁵A. Benvenuti *et al.*, Phys. Rev. Lett. **35**, 1249 (1975).
- ²⁶B. C. Barish *et al.*, Phys. Rev. Lett. **36**, 939 (1976).
- ²⁷M. Holder *et al.*, Phys. Lett. **B69**, 377 (1977).
- ²⁸P. Bosetti *et al.*, Phys. Rev. Lett. **38**, 1248 (1978).
- ²⁹C. Baltay *et al.*, Phys. Rev. Lett. **39**, 62 (1977).
- ³⁰H. Ballagh *et al.*, Phys. Rev. **D21**, 569 (1980).
- ³¹J. Berge *et al.*, Phys. Lett. **B81**, 89 (1979).
- ³²P. Bosetti *et al.*, Phys. Lett. **B73**, 380 (1978).
- ³³N. Armenise *et al.*, Phys. Lett. **B94**, 527 (1980).
- ³⁴J. Blietschau *et al.*, Phys. Lett. **B60**, 207 (1976); **B86**, 108 (1979).
- ³⁵C. Baltay *et al.*, Phys. Rev. Lett. **41**, 73 (1978).
- ³⁶M. S. Atiya *et al.*, Phys. Rev. Lett. **43**, 414 (1979).
- ³⁷D. Aston *et al.*, Phys. Lett. **B94**, 113 (1980).
- ³⁸P. Avery *et al.*, Phys. Rev. Lett. **44**, 1309 (1980).
- ³⁹P. Alibrand *et al.*, Phys. Lett. **B74**, 134 (1978).
- ⁴⁰P. Bosetti *et al.*, Phys. Lett. **B74**, 143 (1978).
- ⁴¹T. Hansl *et al.*, Phys. Lett. **B74**, 139 (1978).

- ⁴²M. Holder *et al.*, Phys. Lett. **B71**, 222 (1977).
⁴³K. Brown *et al.*, Phys. Rev. Lett. **43**, 410 (1979).
⁴⁴A. Diament-Berger *et al.*, Phys. Rev. Lett. **43**, 1774 (1979).
⁴⁵J. L. Ritchie *et al.*, Phys. Rev. Lett. **44**, 230 (1980).
⁴⁶A. Bodek, Sources of Prompt Leptons in Hadronic Collisions. UR 730 COO-3065-253, Rochester, N.Y.
⁴⁷S. Olsen, A. Review of Charmed Particle Production in Hadronic Collisions: UR 750 COO-3065-272, Rochester, N.Y.
⁴⁸W. Allison *et al.*, Phys. Lett. **B93**, 509 (1980).
⁴⁹J. Sandweiss *et al.*, Phys. Rev. Lett. **44**, 1104 (1980).
⁵⁰K. Niu *et al.*, Prog. Theor. Phys. **46**, 1644 (1971).
⁵¹T. Hayashi *et al.*, Prog. Theor. Phys. **47**, 280 (1972).
⁵²K. Hoshino *et al.*, Prog. Theor. Phys. **53**, 1859 (1975).
⁵³H. Fuchi *et al.*, Nuovo Cimento **A45**, 471 (1978).
⁵⁴H. Fuchi *et al.*, Phys. Lett. **B85**, 135 (1979).
⁵⁵N. Ushida *et al.*, Lett. Nuovo Cimento **23**, 577 (1978).
⁵⁶G. Coremans-Bertrand *et al.*, Phys. Lett. **B65**, 480 (1976).
⁵⁷W. Bozzoli *et al.*, Lett. Nuovo Cimento **19**, 32 (1977).
⁵⁸J. Mundra *et al.*, Lett. Nuovo Cimento **18**, 1238 (1977).
⁵⁹P. L. Jain *et al.*, Phys. Rev. Lett. **34**, 1238 (1975).
⁶⁰B. P. Bannik *et al.*, Pis'ma Zh. Eksp. Teor. Fiz. **25**, 586 (1977) [JETP Lett. **25**, 550 (1977)].
⁶¹B. P. Bannik *et al.*, Pis'ma Zh. Eksp. Teor. Fiz. **26**, 399 (1977) [JETP Lett. **26**, 275 (1977)].
⁶²A. Komar *et al.*, Yad. Fiz. **29**, 81 (1979) [Sov. J. Nucl. Phys. **29**, 40 (1979)].
⁶³D. Crenell *et al.*, Phys. Lett. **B78**, 171 (1978).
⁶⁴E. Burhop *et al.*, Nuovo Cimento **39**, 1037 (1965).
⁶⁵E. Burhop *et al.*, Phys. Lett. **B65**, 299 (1976).
⁶⁶A. Read *et al.*, Phys. Rev. **D19**, 1287 (1979).
⁶⁷V. Baranov *et al.*, Yad. Fiz. **27**, 362 (1978) [Sov. J. Nucl. Phys. **27**, 196 (1978)].
⁶⁸N. Ushida, Phys. Rev. Lett. **45**, 1049 (1980).
⁶⁹N. Ushida *et al.*, Phys. Rev. Lett. **45**, 1053 (1980).
⁷⁰R. Ammar *et al.*, Phys. Lett. **B94**, 118 (1980).
⁷¹D. Allasia, Phys. Lett. **B87**, 287 (1980).
⁷²D. Allasia *et al.*, Nucl. Phys. **B176**, 13 (1980).
⁷³C. Angelini *et al.*, Phys. Lett. **B80**, 428 (1979).
⁷⁴C. Angelini *et al.*, Phys. Lett. **B84**, 150 (1979).
⁷⁵M. Adamovich *et al.*, Phys. Lett. **B89**, 427 (1980).
⁷⁶M. Adamovich *et al.*, Phys. Lett. **B99**, 271 (1981).
⁷⁷H. Ballagh *et al.*, Phys. Lett. **B89**, 423 (1980).
⁷⁸N. Ushida *et al.*, Proposal, Ohio State University, May 1980.
⁷⁹S. Amendolia *et al.*, PISA 80-2, 1980.
⁸⁰S. Amendolia *et al.*, PISA 80-1, 1980.
⁸¹Q. Q. Aguilar-Benitez *et al.*, CEN/SPSC/79-80, 1979.
⁸²C. Fisher *et al.*, Proposal CERN/SPS 78-103, 1978.
⁸³T. Cardello *et al.*, FNAL Proposal No. 130, 1980.
⁸⁴H. Fuchi *et al.*, J. Phys. Soc. Japan **47**, No. 3, 687 (1979).
⁸⁵G. Baroni *et al.*, Lett. Nuovo Cimento **24**, 45 (1979).
⁸⁶G. Ingelman *et al.*, Nucl. Instr. and Meth. **165**, 1 (1979).
⁸⁷S. Petrer and G. Romano, Nucl. Instr. and Meth. **174**, 53 (1980).
⁸⁸S. Petrer and G. Romano, Nucl. Instr. and Meth. **174**, 61 (1980).
⁸⁹R. Schindler, Ph. D. Thesis: SLAC Report No. 219, 1979.
⁹⁰W. Bacino *et al.*, Phys. Rev. Lett. **45**, 329 (1980).
⁹¹G. Donaldson, SLAC PUB 2532, 1980.
⁹²T. Hayashi *et al.*, Prog. Theor. Phys. **49**, 350 (1973).
⁹³D. Fakirov and B. Stech, Nucl. Phys. **B133**, 315 (1978).
⁹⁴G. Altarelli *et al.*, Nucl. Phys. **B88**, 285 (1975).
⁹⁵M. Einhorn and C. Quigg, Phys. Rev. **D12**, 2015 (1975).
⁹⁶R. Kingsley *et al.*, Phys. Rev. **D11**, 1919 (1975).
⁹⁷V. Barger *et al.*, Phys. Rev. Lett. **44**, 226 (1980).
⁹⁸T. Kobayashi and N. Yamazaki, Phys. Rev. Lett. **45**, 1070 (1980).
⁹⁹H. Fritsch and P. Minkowski, Phys. Lett. **B90**, 455 (1980).
¹⁰⁰N. Deshpande *et al.*, Phys. Lett. **B90**, 431 (1980).
¹⁰¹I. Bigi and M. Fukugita, Phys. Lett. **B91**, 121 (1980).
¹⁰²W. Bernreuther *et al.*, Z. Phys. **C4**, 257 (1980).
¹⁰³S. P. Rosen *et al.*, Phys. Rev. Lett. **44**, 4 (1980).
¹⁰⁴K. Jagannathan and V. Mathur, Nucl. Phys. **B171**, 78 (1980).
¹⁰⁵J. Prentice, in: 16 Rencontre de Moriond Conference, 1981.

Translated by Clark S. Robinson